Politecnico di Torino

Politecnico di Torino

Environmental and Land Engineering

Corso di Laurea Magistrale in Climate Change

A.a. 2021/2022

Sessione di Laurea Ottobre 2022

Analysis of climate model simulations for evaluating the impacts of AMOC weakening on the Atlantic tropical rainfall in CMIP6 scenario projections

Relatore:

Prof: Jost-Diedrich Graf Von Hardenberg

Co-Relatore:

Prof: Katinka Bellomo

Candidato:

Giada Cerato

Abstract

Thanks to its large-scale teleconnections, the Atlantic Meridional Overturning Circulation (AMOC) plays an active role in shaping the Earth's Climate. Many studies and observations indicate that in recent years the AMOC is undergoing a declining phase. However, although this weakening is supposed to have dramatic consequences all over the globe, regional impacts are still largely unknown. With this work I contribute to improve understanding of the climatic responses of tropical Atlantic precipitation and Hadley atmospheric circulation to an AMOC slowdown. To pursue this objective, I analyze and post-process an ensemble of future projections deriving from eighteen global climate models simulations that belong to the Coupled Model Intercomparison Project 6 (CMIP6).

The analysis confirms the existence of a declining trend for the AMOC, but the large inter-model spread in the AMOC's decline rate leads to a high level of uncertainty. Thus, I split the models in two groups, each one composed of six models: one group includes the models that simulate the strongest decline, while the other includes the models that simulate the weakest decline. Through rigorous statistical testing, I attribute the differences between the two groups to the AMOC's decline impacts. I focus my analysis on the tropical Atlantic, being changes particularly significant in this region. In the group of models with stronger AMOC decline, the annual mean positioning of the ITCZ exhibits a southward shift, whereas the group of models with weaker AMOC decline does not show a southward shift of the ITCZ. To better understand mechanisms of precipitation change, I compute the atmospheric moisture budget. I find that the wind field is the main driver of the equatorial Atlantic moistening occurring in the large AMOC decline group.

The present work helps understanding the impacts of the inter-model spread in the simulation of the AMOC decline, elucidating the mechanisms driving differences in the simulation of future precipitation change in the tropical Atlantic.

Contents

List of Figures

Chapter 1

Introduction

The ocean is an essential element for the Earth's climate system, playing a key role in regulating its dynamics. Thus, understanding its behavior and links with other climate's components is crucial to analyze the possible trajectories that the climate system might undertake in the future. An oceanic region of particular interest is the North Atlantic (NA) Ocean, where the formation of North Atlantic Deep Water (NADW) occurs. NADW is a vital component of the Atlantic Meridional Overturning Circulation (AMOC) [1].

1.1 What is AMOC?

The AMOC is a branch of the global thermohaline circulation (THC), a large-scale oceanic circulation driven by water density gradients, which are in turn controlled by temperature (thermo-) and salinity (-haline). The AMOC transports not only energy (in the form of heat), but also impressive volumes of salty water masses containing carbon and nutrients around the entire Earth's oceanic system, from the Southern Hemisphere (SH) oceans to the Northern Hemisphere (NH) oceans, and back again.

The AMOC itself plays an important role in the North Atlantic ocean (**Figure 1.1** [1]), and is made up of a complex system of surface and deep currents resulting from both thermohalinic and atmospheric drivers. It is responsible for transporting a massive amount of heat (estimated to be annually of the order of 0.5 PW [2]) by

[1] Source: hugo ahlenius unep/grid-arendal

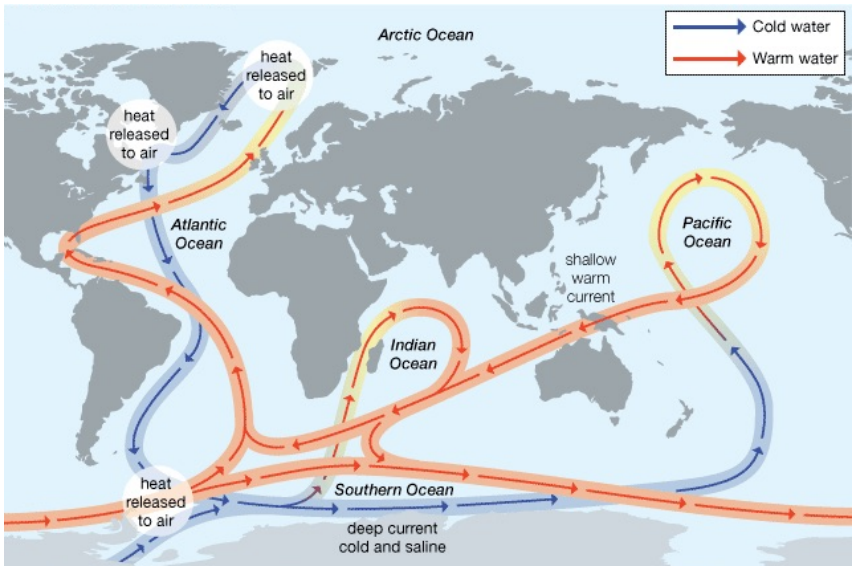

Fig. 1.1 *Schematic illustration of the global thermohaline circulation (THC). AMOC is the branch of the THC that develops in the Atlantic ocean.*

taking up energy at equatorial latitudes and redistributing it among the Northern Hemisphere. In simple words, it originates at tropical latitudes, where a warm flow of water moves northward, at shallow depth (near-surface currents). The warm water masses progressively release heat to the atmosphere while traveling through the North Atlantic basin. When water masses have sufficiently cooled down, and thus density has increased, they sink at higher depth. This sinking process is called deep convection and it is essential in sustaining AMOC, since it connects warm northward currents with deep and cold returning ones [3]. It takes place approximately between 40°N and 60°N. Thus, the near-surface currents are matched by the deep outflow of cold NADW, that travels the way back in southward direction, until it reaches the Southern Ocean and mixes with the rest of World Ocean waters [4].

Figure 1.2 shows the climatology of the Atlantic meridional overturning streamfunction, which is calculated as the zonally integrated meridional velocity field of the water. Thus the integration is performed between the east-west boundaries of the Atlantic ocean, along the latitudinal direction. The lines along which the streamfunction is constant are tangent to the water velocity vectors. In this plot, positive values are associated with a clockwise movement of water volumes. The black arrows help understanding the water motion. The latitudes where contour lines are approximately vertical (between 40°N and 60°N) correspond to those where the

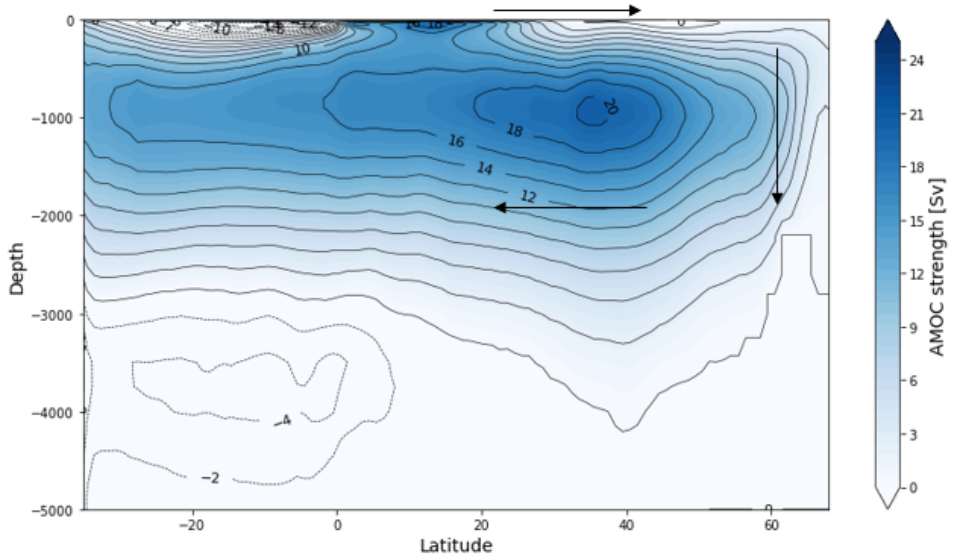

Fig. 1.2 *Transect of Atlantic oceanic streamfunction on a latitude-depth plane. It shows the climatology computed from the historical dataset of all the models (MME). Positive values are associated with a clockwise rotation. The AMOC strength is expressed in Sv (1 Sv = 10^6 $\frac{m^3}{s}$).*

sinking process occurs, forming the NADW. Then, cooled water masses reverse their traveling direction.

The northward surface heat fluxes that generate over the North Atlantic ocean have an important thermoregulator effect on the climate system of the Northern Hemisphere. For instance, continuous heat released in the subpolar North Atlantic is thought to be the greatest contribution to the mild climate typical of northwestern Europe [2].

1.2 AMOC vulnerability to Climate Change and possible consequences

The AMOC is sensitive to climate change, since both temperature and salinity might be affected by it. In the last century, warmer surface water and North Atlantic ocean freshening induced by sea ice melting, may have weakened the AMOC [3]. Warmer surface water temperature reduces the thermodynamic driver of AMOC, by reducing the oceanic temperature gradient between the equator and the pole, and thus making

it harder for the NA oceanic near-surface currents to release heat to the atmosphere. Typically, this process is fundamental for increasing water density and allowing the convective sinking in the NA. A freshening of the northern North Atlantic ocean would instead reduce the upper-ocean salinity, and thus density. This occurs especially in the Labrador Sea, where Greenland and Arctic gates freshwater runoff tends to converge. As a consequence of both the phenomena, water stratification increases, thus inhibiting water downwelling and weakening the mechanism of deep convective mixing [5] that typically plays a major role in sustaining the bottom branch of the AMOC. [6]

An AMOC weakening trend is confirmed by recent direct observations that suggest it is facing a declining phase. However, determining its magnitude in a precise manner is still challenging due to the high degree of AMOC variability and short duration of the observations that only began in April 2004 from the RAPID/MOCHA array, monitoring the oceanic current at 26°N in the Atlantic. Thus, there is large debate regarding AMOC evolution in recent years, and further ambiguity related to its fate at the end of the century. [6] Coupled ocean-atmosphere numerical models' simulations confirm the existence of a declining trend and set the beginning of it around late 1990s [2]. With the ongoing land ice melting, especially from the Greenland ice sheets, scientists believe a further slowdown is "very likely" to happen in the coming decades. Also future projections indicate that this trend is going to continue during the current century, under the influence of anthropogenic warming. In a changing climate, a declining AMOC has the main effect of buffering the surface warming, slowing down the process and thus delaying the full extent of global surface warming [7].

To understand the possible evolution of the AMOC, in 1961 Stommel developed an idealized ocean box model. In simple words, the model mimics the oceanic circulation strength as a function of density differences, which in turn are affected by both temperature and salinity. This simple model demonstrates the existence of multiple AMOC's equilibria. One equilibrium state in which AMOC is strong and similar to the actual dynamics, and another one in which AMOC is extremely weak, or even reversed. Crossing the stability threshold can lead to an abrupt oceanic circulation change.

Besides modeling studies, also paleoclimate reconstructions and other studies raise concerns about an AMOC irreversible shutdown, identifying the AMOC as

a tipping element of the climate system [8]. In the past, abrupt climate changes such as the massive temperature shift that occurred during the Dansgaard-Oeschger events ([9], [10], [11]), have been linked to AMOC variations. In fact, since usually AMOC brings salty warm water at the higher latitudes, its slowdown may trigger a positive feedback mechanism by reducing the salinity transport and thus amplifying the freshening over the North Atlantic sector [3], with the overall consequence of inducing an acceleration in the slowdown process.

Many studies using climate model simulations have examined this possibility and the related consequences by adding distributed freshwater pulses into broad or narrow regions in the North Atlantic basin (in the so-called water hosing experiments), artificially inducing the AMOC to collapse. Global consequences are expected if an AMOC collapse occurred, including an estimated surface air temperature reduction up to 10°C in the North Atlantic basin [2]. However, according to the last International Panel on Climate Change AR5 report, an AMOC shutdown has potentially high impacts, but it is "very unlikely" to occur in the 21st century. [3] Unlike other studies, Bellomo et al. (2021) uses an ensemble of CMIP5 and CMIP6 models to analyze the AMOC response to the $4xCO_2$ experiment, and the related climate system responses. In those simulations the AMOC does not collapse, but progressively weakens, until reaching a weak but stable strength.

1.3 Main AMOC's teleconnections

The AMOC is known to be closely connected with many other components of the climate system, and its weakening impacts would spread worldwide, resulting in complex large-scale patterns of change.

Basin-scale measurements of the Sea Surface Temperature (SST) performed over time in the North Atlantic ocean show repetitive cycles with multidecadal occurrence. SST anomalies over the NA flip their sign with an observed period between 60 and 80 years. This mode of natural variability can be, at least in part, associated with AMOC fluctuations. These repetitive cycles have traditionally been called Atlantic Multidecadal Oscillation (AMO). However, recent studies suggest that the NA variability is not composed by only one oscillation at fixed frequency, but rather by a broad band of low-frequency signals, thus it would be more pertinent to refer to as Atlantic Multidecadal Variability (AMV) [1]. Since the AMOC is partly

atmospheric-driven, a notable contribution to its variability comes from the North Atlantic Oscillation (NAO), an irregular atmospheric sea-level pressure fluctuation. Positive and negative NAO phases are linked with anomalous jet streams and storm tracks over the NA, modulating the Atlantic meridional heat and moisture transport.

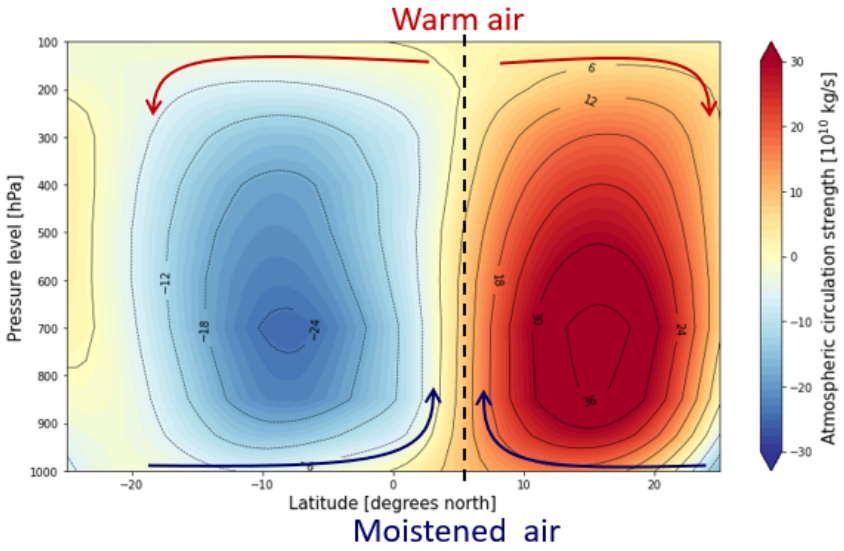

Fig. 1.3 *Climatological mean annual air streamfunction (Hadley cells) computed from the historical dataset of all the models. Positive (negative) values represent air masses clockwise (anti-clockwise) rotation.*

Another example of AMOC's teleconnection is the close relation it has with the Hadley atmospheric circulation, which not only dominates the regional climate in tropics and sub-tropics, but also shapes the global distribution of precipitation, clouds and humidity ([12], [13]). The Hadley circulation is a system of air cells, where heated air masses rise near the equator, then stop rising underneath the tropopause while moving poleward. Air progressively cools down and sinks at around 30°N (mean annual position). By redistributing energy between the Hemispheres, the AMOC causes an hemispheric oceanic heat transport (OHT) imbalance. The Hadley circulation counteracts with an anomalous atmospheric heat transport (AHT), strengthening and expanding the Southern Hemisphere Hadley cell. In fact, the Hadley circulation acts in order to compensate for the AMOC's heat uptake in the SH, by transporting more energy from the Northern Hemisphere to the Southern one. This phenomenon is accomplished by a cross-equatorial heat transport, operated by

an anomalous Hadley cell in the Southern Hemisphere. Also a general bulk annual northward shift of the Hadley cells exists (see **Figure 1.4** [2]). [14]

Note that this analysis only deals with energy exchanges occurring over the Tropical Atlantic region, thus the cross-equatorial Hadley cell has the consequence of transporting more heat southward on a regional scale. On a global scale, the overall atmospheric energy transport is positive towards the pole (as well as the OHT), as a consequence of an imbalance between the energy absorbed at the equator and the energy released at the pole.

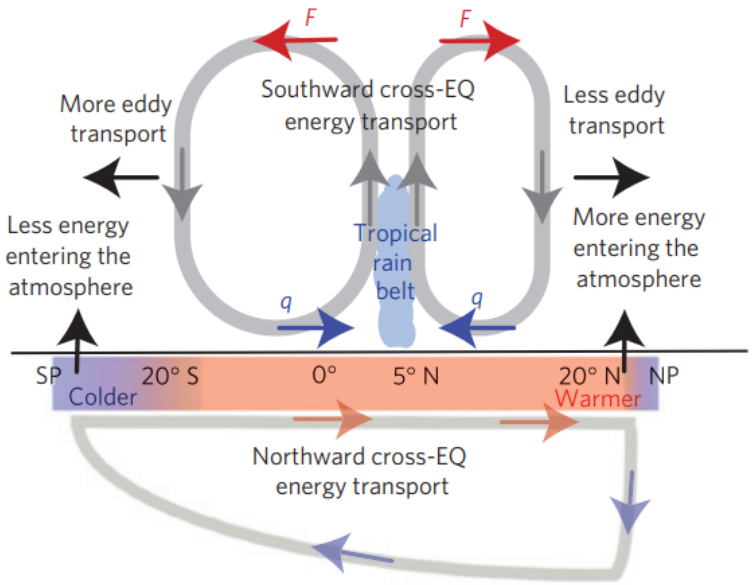

Fig. 1.4 *Schematic illustration about how the AMOC influences the Hadley circulation which in turn pushes the ITCZ northward.*

Whereas the heat transport (motion of warm air) occurs through the upper limb of the Hadley cell, the lower limb is responsible for transporting dry air that absorbs moisture while moving towards the equator. The moistened air mass thus converges into the ascending branch of the cell, giving rise to the so-called Intertropical Convergence Zone (ITCZ). The ITCZ is a narrow zonal band characterized by low pressure and high precipitation intensity, responsible for shaping the largely wet hydrological regime in the Atlantic deep tropics, between South America and the west coast of Africa. As we can see in **Figure 1.3**, the bulk northward shift of the Hadley cells affects the positioning of the ITCZ, thus being dragged North of the equator, and

[2] Source: Frierson, D., Coauthors. Contribution of ocean overturning circulation to tropical rainfall peak in the Northern Hemisphere. Nat. Geosci. 6, 940–944 (2013).

localized in proximity of the black dashed line ([2], [14], [15]). As a result, the current mean annual intensity peak of tropical Atlantic precipitation sits at about 5°N. **Figure 1.5** confirms that our models' historical simulations well represent in the Atlantic Ocean the north of the equator position of the ITCZ, which corresponds to the blue band that extends between the Brazilian coast and western Africa, just above the equator. In the Pacific Ocean models tend to simulate a double ITCZ, also known as the double ITCZ bias. However, this bias is smaller in the CMIP6 models compared to their predecessors in the CMIP5 archive.

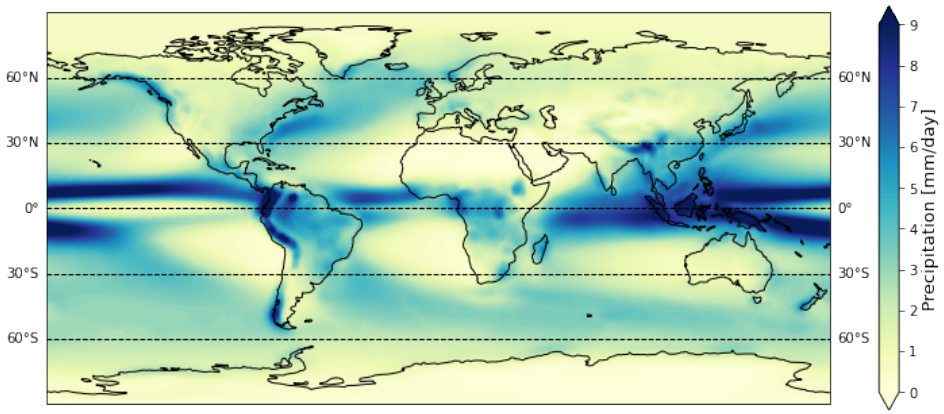

Fig. 1.5 *Precipitation climatology computed from the historical datasets of all the models.*

1.4 Expected climate responses to an AMOC decline and aim of the study

Because it plays a major role in shaping the global climate, any disruption or change in the AMOC's dynamics may have dramatic consequences. The impacts of an AMOC slowdown are not expected to be confined to the North Atlantic [16], but to be widely spread all over the globe, and to involve a number of climate essential variables, with important societal and economic implications. However, the existence of NADW formation and its connection with surface currents makes the AMOC an exceptionally difficult mechanism to model [1]. This makes the models' predictive skills about the AMOC evolution affected by a high level of uncertainty. Hence, a deep understanding of AMOC-related impacts is limited by the scarcity of

available direct observational data and biases in the model simulations. Due to those limitations, a further effort is needed to analyze the impacts of an AMOC decline.

In future climatic projections, the reduced poleward heat transport caused by an AMOC slowdown is thought to be the greatest contributor to the rise to the North Atlantic Warming Hole (NAWH). The NAWH is a region of modest dimension located in the northern North Atlantic that is supposed to warm at a slower rate than the rest of the globe ([17], [18]). **Section 3.1** provides a study of the SST response to an AMOC decline under the SSP585 scenario, and demonstrates that in CMIP6 models the NAWH rises as a consequence of a strong AMOC decline. Furthermore, several previous studies ([14], [15], [19]) have suggested that models generally predict a southward ITCZ shift following an AMOC's collapse (or slowdown). This phenomenon has been attributed to the reduction in cross-equatorial oceanic heat transport, which induces cooling of the Northern Hemisphere, and thus induces a weakening of the southward atmospheric heat transport [20], which in general is operated by the cross-equatorial SH Hadley cell. The possibility of an ITCZ shift as a consequence of an AMOC decline is analyzed in **Section 3.2**, while the coherent Hadley circulation variations are investigated in **Section 3.3**.

Since regional impacts of an AMOC slowdown are still largely unknown, with this thesis I build upon our knowledge of AMOC-driven impacts on tropical precipitation and atmospheric circulation. This work is inspired by the analysis performed by Bellomo et al. (2020). The study evaluates the AMOC decline impacts under the $4xCO_2$ experiment, which forces the climate models simulations with a quadrupled CO_2 concentration in the atmosphere with respect to the preindustrial climate. Here, instead, I analyze the climate system response to the AMOC decline that is projected to occur by the end of the current century under the SSP585 scenario projection. To fulfill this purpose, I use 18 models belonging to the Coupled Model Intercomparison Project 6 (CMIP6). Since the NA climate is extremely complex to simulate, the AMOC strength representation and its reduction rate largely vary into my sample of models. Due to the large inter-model spread in AMOC's representation, I assessed the AMOC's role in future climate change by forming two groups of models. One includes the models that simulate the weakest AMOC decline, while the other group includes the models that simulate the strongest AMOC decline. Thus, making a comparison between the ensembles of future projections predicted by the two sets of models, I find the main differences between the climate system response to a weak AMOC decline and to a strong AMOC decline. I perform rigorous statistical

testing, and when the differences between the two groups' future projections result to be statistically significant (above 95%), I argue that these differences are driven by the difference in AMOC slowdown between the two groups of models. This methodology is proven to be robust, as demonstrated in Bellomo et al. (2021).

Chapter 2

Models and Datasets

2.1 CMIP6 climate models and state of the art

Climate and Earth system models are extremely complex and sophisticated computer codes that allow us to understand and simulate past, present, and future climate dynamics. A climate model is sort of a virtual Earth, trying to mimic processes and feedback that regulates the real world's climate system. This is performed by using mathematical differential equations based on the laws of physics, fluid motion and chemistry, that describe how heat, moisture, momentum, and chemicals move across space and through time [1]. Climate models use three-dimensional grids of cells, with different types of horizontal and vertical resolution [2]. The mathematical equations are solved at each point of these grids, and information is passed to the neighboring cells, to model the mass and energy exchange over time. In the context of climate change, models are extremely useful tools, as they are used to predict the future climate. Thus climate modeling represents one of the most important resources for our society to get reliable and high-quality climate information, being also a useful decision-making support tool.

The models I use belong to the Coupled Model Intercomparison Project 6 (CMIP6), whose aim is to improve scientific knowledge about the climate system, performing coordinated experiments and taking advantage of the collaborative work of more than 40 modeling centers. The outputs of the simulations differ because

[1] https://climate.copernicus.eu/latest-projections-future-climate-now-available

[2] https://www.climate.gov/maps-data/climate-data-primer/predicting-climate/climate-models

the climate models are different. CMIP6 intervenes with the aim of harmonizing the experiments conducted by each modeling group, by setting up the models' inputs in the same way, and constraining their simulations with the same sets of external forcings. A collaborative multi-model framework is of extreme importance to address the issue of structural uncertainty in model's design and climatic internal variability. By collectively analyzing climate outputs and performing Multi-Model Ensembles (MMEs) scientists can get information about a full range of possible future climate assets and evaluate the related uncertainties. Furthermore, MMEs are proven to increase the reliability, predictability and consistency of model's output [21]. The Sixth generation climate models introduce some new features with respect to the previous ones, such as higher levels of resolution and modelization of additional processes.

Letters CM of the acronym CMIP stand for Coupled Models, and express the fact that these models include most components of the climate system (such as biosphere, atmosphere, oceans, land surface, and so on), and make them able to interact with each other, with a two-way communication. The passage of information between different subsystems is extremely complicated, since the communicating components codes are completely disjointed, and thus may differ in spatial and temporal resolution [3].

For my thesis I put a major focus on the atmosphere's and the ocean's subsystems, to get information about how they communicate with each other, and understand the influence an AMOC slowdown may have on the Atlantic tropical precipitation and atmospheric circulation patterns. However, as mentioned above, an AMOC rigorous computerization is difficult, due to the complexity in representing the energy and mass exchange occurring between near-surface currents and NADW, the heat fluxes between shallow water and overlying atmosphere, as well as the wind-driven mechanisms affecting AMOC. Also the Atlantic Multidecadal Variability and the North Atlantic Oscillation are climate phenomena difficult to be accurately represented, thus giving an additional source of uncertainty. As we have explained in the previous section, freshwater fluxes from sea-ice melting are supposed to play a role in weakening the AMOC. However, the physical processes associated with the sea-ice contribution to the AMOC decline are still unclear in comprehensive fully coupled models ([22], [23]). As we will see later, all these factors contribute to a

[3] https://www.cesm.ucar.edu/models/ccsm3.0/cpl6/usersguide/node16.html

non-accurate representation of the AMOC historical mean state, its natural variability, and sensitivity to anthropogenic forcings, leading to a large inter-model spread. [2] Kim et al. (2018) argues that many CMIP6 models still largely underestimate the AMV, influencing the simulated AMOC response to anthropogenic forcings or even its stability, and thus increasing uncertainties on the representation of the fate of AMOC for the next future [2] and on AMOC-induced climate changes.

For this study I use the historical simulation, which spans the period between 1850 and 2014. These simulations are used to assess the models' performance, by checking if they faithfully emulates the past climate. After evaluating the performance of the models, they can run under different standardized sets of forcings, simulating scenarios which are relevant to societal concerns about climate change, thus being extremely useful for climate research. The available future scenarios, which are analyzed in detail in O' Neill (2016), define possible future developments of anthropogenic drivers of climate change, together with consistent socioeconomic developments.

For my analysis, amongst all the simulations, I use the SSP585 (Shared Socioeconomic Pathway 5) climate projection scenario, whose radiative forcing is close to the one of the old RCP8.5 scenario of the CMIP5 (amongst the others, it is the only one that reaches radiative forcing of 8.5 $\frac{W}{m^2}$ by 2100) [24]. It is also known as the high-emissions scenario. It describes the future greenhouse gas concentration rise caused by a society that strongly relies on fossil fuels, has a weak development of renewable energies and no mitigation policies are applied. **Figure 2.1** [4] shows how the CO_2 concentration in the atmosphere is expected to progressively increase under the energy-intensive SSP585 scenario. The simulated CO_2 concentration in the atmosphere grows exponentially, almost reaching 1100 ppm by 2100.

The SSP future simulations span the period between 2015 and 2100 (or 2300 for some extended simulations), and here are used to understand the climatic anomalies that might arise by the end of the current century, under a sort of business-as-usual scenario.

[4] Source: O'Neill et al. The Scenario Model Intercomparison Project (ScenarioMIP) for CMIP6 (2016)

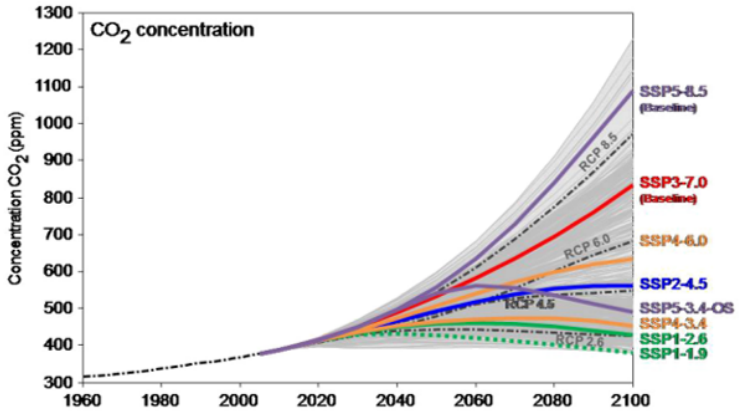

Fig. 2.1 *CO_2 concentration in atmosphere under SSP scenarios of development.*

2.2 Materials

As previously mentioned, to fulfill the objective of this work I use an ensemble of 18 coupled ocean-atmosphere numerical models belonging to the Coupled Model Intercomparison Project 6. Amongst all the new generation models, I settled on those models that have submitted the stream function variable in the North Atlantic basin, for both the historical simulation and the SSP585 future projection. Overall, the collected dataset spans the period between 1850 and 2100, with monthly temporal resolution.

When available, I use the r1i1p1f1 ensemble member. The only exceptions are: r1i1p2f1 for CanESM5-CanOE, r10i1p1f1 for CESM2, and r1i1p1f2 for GISS-E2-1-G, because for the variant r1i1p1f1 the stream function for SSP585 run was not available. These may differ from other ensemble members of the same model in the physics ("p") or in detailed forcing used ("f").

I select the following variables to conduct the analysis: overturning streamfunction (msftmz), temperature at the surface (tas) that over the ocean corresponds to the Sea Surface Temperature, mixed layer depth (mlotst), precipitation (pr), evaporation (evspsbl), zonal wind (ua), meridional wind (va), sea level pressure (ps) and specific humidity (hus).

Table 2.2 provides a complete list of the models that make up my sample, together with the institution that released the model, the ensemble member and the spatial resolution.

Table 2.1 List of models used for the study, modelling centre, variant label, model's resolution

Models	Modelling centre	Variant label	Resolution
ACCESS-CM2	CSIRO-ARCCSS (Australia)	r1i1p1f1	1.875° × 1.25°
ACCESS-ESM1-5	CSIRO-ARCCSS (Australia)	r1i1p1f1	1.875° x 1.25°
CanESM5	Canadian Centre for Climate Modelling and Analysis	r1i1p1f1	42.8° × 2.8°
CanESM5-CanOE	Canadian Centre for Climate Modelling and Analysis	r1i1p2f1	2.8° x 2.8°
CAS-ESM2-0	Chinese Academy of Science	r1i1p1f1	1.4° x 1.4°
CESM2	National Centre of Atmospheric Research (USA)	r10i1p1f1	1.25° x 0.94°
CESM2-WACCM	National Centre of Atmospheric Research (USA)	r1i1p1f1	1.25° x 0.94°
FGOALS-f3-L	Chinese Academy of Science	r1i1p1f1	0.625° x 1°
FGOALS-g3	Chinese Academy of Science	r1i1p1f1	2° x 5°
GISS-E2-1-G	NASA Goddar Institute for Space Studies	r1i1p1f2	2.5° x 2°
INM-CM4-8	Institute of Numerical Mathematics (Russia)	r1i1p1f1	2° x 1.5°
INM-CM5-0	Institute of Numerical Mathematics (Russia)	r1i1p1f1	2° x 1.5°
MIROC6	MIROC6 (Japan)	r1i1p1f1	1.4° x 1.4°
MPI-ESM1-2-HR	Max Planck Institute for Meteorology (Germany)	r1i1p1f1	0.94° x 0.93°
MPI-ESM1-2-LR	Max Planck Institute for Meteorology (Germany)	r1i1p1f1	1.875° × 1.85°
MRI-ESM2-0	Meteorological Research Institute (Japan)	r1i1p1f1	1.125° × 1.121°
NorESM2-LM	Norwegian Climate Centre (Norway)	r1i1p1f1	2.5° x 1.9°
NorESM2-MM	Norwegian Climate Centre (Norway)	r1i1p1f1	0.25° × 0.94°

2.3 Methodology

2.3.1 Pre-processing of the data

Before performing the analysis, all the datasets have been pre-processed, using the Climate Data Operators (CDO) tool on a linux machine. The package has been released by the Max Planck Institute for Meteorology, and contains a collection of command line operators that can be used for performing standard processing of climate data, in a fast and easy manner.

All the different models' outputs have been spatially interpolated with a bilinear interpolation on a common grid before performing the analysis.

- All the two-dimensional datasets' horizontal grids are interpolated onto a regular gaussian grid with a resolution of 0.75° x 0.75°. This is close to the highest resolution present in the models ensemble.
- The atmosphere's three-dimensional variables (ua, va, hus, ps) have a horizontal resolution of 0.75° x 0.75° as well, and 17 vertical levels, with increasing size from from 1000 hPa to 100000 hPa.
- The overturning stream function variable (msftmz) datasets have been interpolated on a common depth grid composed of 40 levels with a thickness of 5m at the surface and increasing to 250 m at a depth of 5500 m.

Datasets have also been cut to focus on the time spans of interest. For the historical run, years between 1971 and 2000 are selected to represent an average past condition, when the decline was at the very beginning, or, depending on the specific model, even had yet to occur. Thus, years before 2000 are used as a comparative term representing the actual normal condition. Years between 2071 and 2100 are selected to represent the future condition at the end of the current century for each model. All the historical run (future projections) variables datasets are thus cut to shorter datasets spanning the years 1971/2000 (2071/2100).

For each model I perform a two-tailed t-test with a significance level of 95% on the anomalies between the temperature field in the historical dataset and the temperature field predicted by the future one. The procedure is used to exclude the possibility that such anomalies derive from the Earth system's natural variability and

safely assess that they are the consequences of a changing climate. The tests revealed that in some models, a few small regions experience a temperature change that is not statistically relevant. All the results and a brief explanation are provided in **Appendix A**. The same procedure has been applied on the precipitation anomalies, with a significant level threshold slightly lower (80%), given the highly dishomogeneous spatial distribution of precipitation anomalies.

2.3.2 AMOC time series and subdivision of the models

Figure 2.2 shows the time series of AMOC decline predicted by our ensemble of models, with average annual values. To quantify the AMOC's intensity variation, I calculate the difference between the time-averaged intensity over the historical period (1971 - 2000) and over the future one (2071 - 2100). The intensity of AMOC has been retrieved as the maximum value of the overturning stream function variable in the North Atlantic basin, between 30°N and 50°N, and below 500m of depth. All the models' time series have been smoothened for a better visualization using a running mean of 7-years (low-pass filter), although the multidecadal oscillations can still be seen for several simulations.

Under increasing greenhouse gas concentration in the SSP585 experiment, all the models predict a declining trend in AMOC's strength. The precise beginning of the decline is uncertain, but models mainly locate it in the second half of the 20th century. An intensification of the decline rate occurs around the late 1990s, and continues over the current century. The large inter-model spread in AMOC's representation that we have already discussed is visible both in the historical simulation and in the future projection. In fact, simulated historical strength ranges between mean values of 14 Sv and 29 Sv, depending on the specific model. Such uncertainty further spreads in the future projections.

For the analysis I exploit this inter-model spread using the same approach suggested by Bellomo et al. (2021), thus comparing climate responses of an ensemble of models where the simulated AMOC decline is large, to another ensemble composed by models that simulate a smaller AMOC decline. As a very first step, I divide the models in order to form two groups composed of six models each (one third of the total number of models). The first group includes the models that predict the lowest

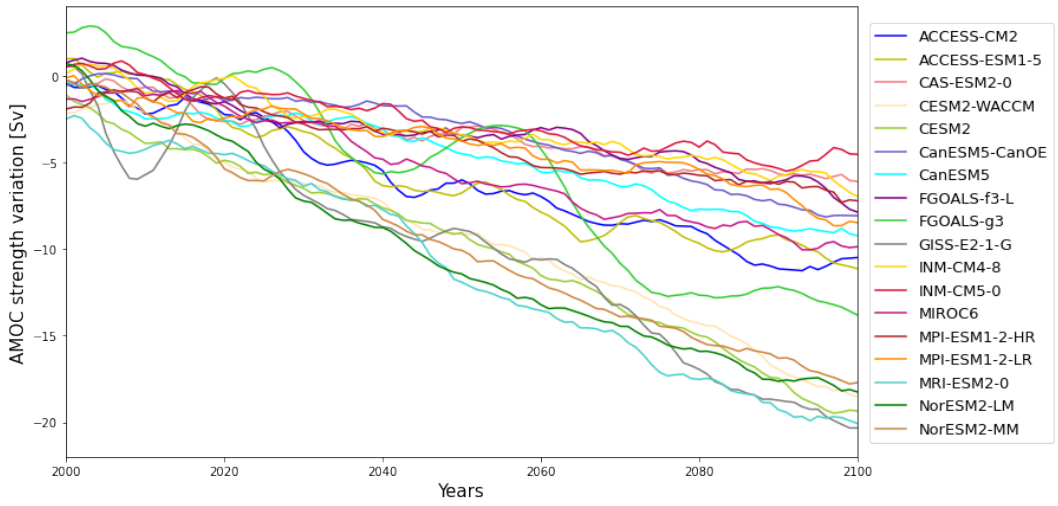

Fig. 2.2 *Time series of AMOC reduction over the 21st century with respect to the averaged intensity calculated over the historical time span. A 7-year running average has been applied for a better visualization.*

AMOC intensity reduction, and the second one is made up of the models that predict the strongest AMOC intensity reduction over the period of one century.

The AMOC reduction for each model is simply retrieved as the difference between the average value in the future dataset minus the average value in the historical one, and it is employed as discriminating criteria in choosing the members of the two groups.

The six models that exhibit the strongest (weakest) AMOC's strength reduction are classified as "Large (Small) AMOC decline", here abbreviated as SAD and LAD, respectively.

- For the small AMOC decline group the predicted weakening ranges between -5 and -7 Sv (-25% and -33%). Included models are: CAS-ESM2-0, FGOALS-f3-L, INM-CM4-8, INM-CM5-0, MPI-ESM1-2-HR, MPI-ESM1-2-LR.
- For the large AMOC decline group the predicted weakening ranges between -16 and -18 Sv (between -61% and -74%). Included models are: CESM2-WACCM, CESM2, GISS-E2-1-G, MRI-ESM2-0, NorESM2-LM, NorESM2-MM.

The division is based on reductions in Sverdrups Sv (1 Sv = 10^6 $\frac{m^3}{s}$), but it would have been the same if instead I used the reduction expressed in percentage.

Table 2.2 *AMOC intensity variation (column 4 and 5) calculated as the difference between the mean historical intensity (second column) and the intensity predicted by the end of the century (third column). The former (latter) six models are those models that provide the lower (stronger) AMOC's intensity reduction. The last column shows the percentage of variation. Average value of intensity reduction is -11 Sv (-47 %))*

Models	Historical mean [Sv]	Future mean [Sv]	Reduction [Sv]	Reduction [%]
INM-CM5-0	18.1	13.5	-4.6	-25%
INM-CM4-8	19.1	13.5	-5.6	-29%
FGOALS-f3-L	25.3	19.3	-6.0	-24%
CAS-ESM2-0	20.4	15.1	-6.1	-28%
MPI-ESM1-2-HR	19.0	13.2	-6.3	-33%
MPI-ESM1-2-LR	21.9	15.2	-7.1	-31%
CanESM5-CanOE	14.3	7.2	-7.2	-50%
CanESM5	15.5	7.2	-8.3	-54%
MIROC6	17.4	8.4	-9.0	-52%
ACCESS-CM2	22.5	12.3	-10.2	-45%
ACCESS-ESM1-5	24.2	14.2	-10.4	-42%
FGOALS-g3	34.3	21.3	-13.3	-38%
CESM2-WACCM	26.5	10.3	-16.2	-61%
NorESM2-MM	26.2	10.0	-16.2	-62%
CESM2	27.1	10.0	-17.1	-63%
NoeESM2-LM	26.2	9.21	-17.4	-65%
GISS-E2-1-G	29.3	11.3	-18.4	-63%
MRI-ESM2-0	25.1	6.44	-19.1	-74%

Generally, models with stronger (weaker) AMOC in the mean climate also undergo a stronger (weaker) AMOC reduction, thus generally belonging to the large (small) AMOC decline group. This tendency has already been pointed out in previous studies ([25], [2]). The cross sections reported above show the ensemble mean of the streamfunction variation in the North Atlantic basin for the two groups. Black contour lines correspond to the ensemble mean climatology for the two sets of models and confirm the aforementioned hypothesis, showing higher values of historical AMOC intensity for the LAD group. Note that the streamfunctions demonstrate that the strength reduction occurs at all the latitudes in the North Atlantic ocean, despite the AMOC intensity has been evaluated in only one point. In general, the largest variations occur between 25°N and 40 °N, in agreement with Bellomo et al. (2021)

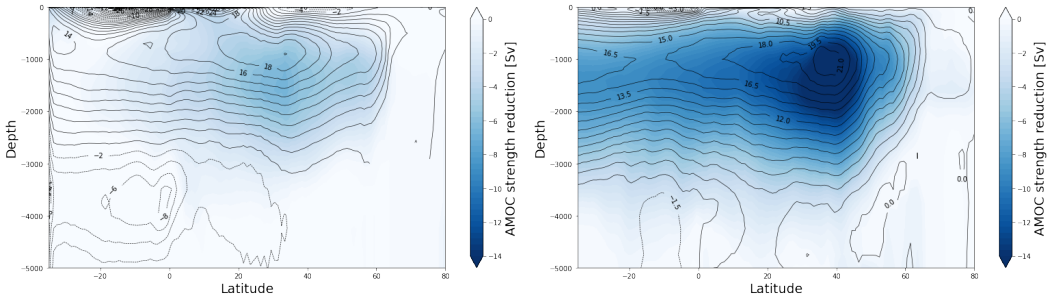

(a) (b)

Fig. 2.3 *Atlantic overturning streamfunctions variation between historical run and future projection for a) SAD group and b) LAD group. Superimposed black contour lines represent the mean annual climatology for the two sets of models.*

None of the investigated models predicts a complete AMOC shutdown in the next decades, because at most AMOC reduces to 6 or 7 Sv, excluding this possibility under the SSP585 scenario. As already mentioned, the SSP585 scenario represents the "worst-case scenario", thus further confirming the very low probability of a total collapse to occur in the current century. However, AMOC declines range between 25% and 74%, thus even if the possibility of an AMOC collapse is averted, the projected intensity reductions are still very significant. Bellomo et al. (2021) demonstrate that an AMOC shutdown does not occur even when models are abruptly forced with quadrupled CO_2 concentration with respect to the preindustrial climate. Moreover, for some models the SSP585 projections are available until 2300 (here are not shown because the run was not available for each model) and reveal that the AMOC intensity is likely going to reach a plateau, as a prolonged state of AMOC minimum [7]. In these simulations AMOC stabilizes its strength during the second

half of the 22^{nd} century. Thus, a weaker but stable system of oceanic currents is expected to continue existing within the North Atlantic Ocean. However, it should be mentioned here that according to Liu et al. (2019), the AMOC collapse in a warming climate may be an overlooked possibility in CMIP climate models.

In the study conducted by Bellomo et al. (2021), the large AMOC decline models are associated with a stronger mixed layer reduction in the Labrador Sea with respect to small AMOC decline models. Consistently, our sample's future projections reveal a larger decrease of the Mixed Layer Depth (MLD) associated with the strong AMOC decline scenario with respect to the small one. However, the picture is not shown here since values for some models were missing, thus leading to a MME for the SAD group composed of only 4 models, but can be seen in **Appendix C**. The thinning of MLD in the Labrador sea occurs due to increased stratification operated by the freshening of the near-surface water, thus the water column stabilizes, inhibiting the deep convection that usually sustains the lower branch of the AMOC.

2.3.3 Anomalies maps

The analysis of future projections is the focus of my thesis. We can visualize and measure the climate response to a slowdown of AMOC by computing the anomalies that are projected to arise over the period of one century, between the future scenario and the historical experiment. To do so, I proceed as follows.

First, I compute the time means of the simulations to obtain two spatial maps representing the averaged past (ensemble mean over the historical dataset) and averaged future climate conditions (ensemble mean over the future dataset). These maps are then subtracted to each other, to obtain anomalies maps. Field means are extracted from the TAS datasets, to measure the global temperature variation (Global mean Surface Air Temperature variation, ΔGSAT) predicted by each model and then used to normalize our anomalies maps. The normalization is computed for each variable of each individual model at each grid point. The procedure is done because each model has its own climate sensitivity, which depends on how much the climate warms as a response to a given forcing (in this case the greenhouse gas concentration rise) [26]. This normalization makes the models independent from their climate sensitivity, and ensures that climate responses deriving from other processes and feedback are excluded. Thus, it allows us to safely assess that the detected climate

anomalies are a response to the weakening of the AMOC. The normalization also makes the comparison between the maps and with other similar studies easier. As demonstrated by Bellomo et al. (2021), ΔGSAT itself is slightly dependent on the AMOC variation, but being the inter-model spread large and the correlation between ΔGSAT and ΔAMOC relatively low, it is possible to argue that ΔGSAT is mostly determined by other climate feedback.

Being in a multi-model framework, the individually normalized anomalies maps are then averaged across the sets of models (MMEs).Two ensembles means are thus performed: one including all the models classified as small AMOC decline (SAD) and one including those classified as large AMOC decline (LAD). As a result, we get two different spatial maps (one for the small decline group and one for the large decline group) where each grid point represents the variable average change normalized per degree of global warming. As a last step, I subtract the anomaly map predicted by the LAD group and the one predicted by the SAD group (large AMOC decline minus small AMOC decline). This procedure highlights the differences between the future climate predicted by the two sets of models. The resulting map can be interpreted as the expected impact that a larger AMOC decline may cause in the future climate change, with respect to a weaker decline. [25]

A two-tailed t-test with significance level of 95% assuming equal variance is used to understand whether the differences between the normalized anomalies predicted by the two sets of models are statistically relevant. Following the example of Bellomo et al. (2021), where these tests return a sufficiently high significance level, I argue that the differences between the groups are driven by the difference in AMOC decline between the two groups. To further confirm the statistical significance of the anomalies, I form two groups of 500 samples of randomly picked groups of six models among the 18 under study, without repetition. A bootstrap test is performed to further check whether differences between the two sets of models (LAD and SAD) are statistically different from the 500 differences of the two randomly chosen groups. The differences are evaluated in absolute value, and when the differences between LAD and SAD groups fall in the 5% tail of the distribution, I assume they are statistically relevant. Only results obtained with this second method are shown in this work, because they largely agree with the two tailed t-tests described above.

Chapter 3

Results

3.1 Surface air temperature anomalies in response to an AMOC decline

As briefly explained in the introduction, the main drivers of the North Atlantic SST variability are the oceanic heat transport and atmosphere-ocean heat fluxes, which are both influenced by AMOC variability [27]. During the positive phase of the AMV, a strong AMOC is associated with an anomalous warming over the North Atlantic region and a weaker cooling over the South Atlantic region, caused by positive northward meridional oceanic heat transport anomaly. In contrast, during a negative AMV phase, the SST anomalies over the NA ocean flip sign. This behavior resembles the interhemispheric asymmetric SST response to a negative northward meridional heat transport anomaly caused by a simulated AMOC collapse, as pointed out by Zhang et al. (2019).

In this section I analyze the North Atlantic SST temperature response to a changing climate, and in particular its response to a progressive AMOC slowdown. Since the SST response to an AMOC collapse is similar to the SST response to a prolonged negative phase of the AMV, I expect that SST anomalies resulting from a weakening of the North Atlantic meridional oceanic heat transport result in recognizable large-scale patterns of change as well. [2]

Generally speaking, under the high emission SSP585 future scenario all the models predict an overall dramatic increase of near-surface temperature, resulting

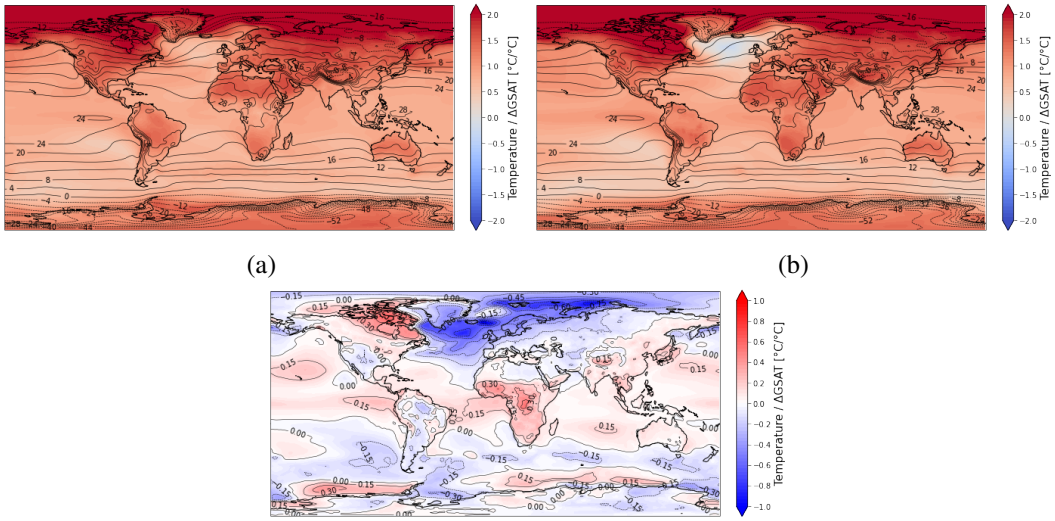

Fig. 3.1 *Temperature anomalies for a) SAD group and b) LAD group. Superimposed black contours represent the mean climatology computed from all the 18 models. The temperature variation predicted by each models is normalized by the respective ΔGSAT, thus units of measure are °C per degree of global warming. Figure c) is the difference between a) and b). Stippling indicates where the difference between LAD and SAD groups is statistically significant at the 95% threshold.*

in an averaged global warming that ranges between 3°C and 5°C, depending on the specific model. For both groups, the surface air temperature change shows the gradient of warming decreasing from Northern high latitudes to the Southern Hemisphere [21], ending up at Antarctic latitudes where the gradient increases again a little.

A land-ocean warming contrast is evident. In fact, the continents warm faster with respect to the oceanic regions. This phenomenon happens due to the higher thermal capacity of the ocean, which is also the reason why oceanic regions are considered important thermoregulators for the whole climate system, accumulating heat and slowing down the process of global warming. The only few exceptions to this trend are the desertic regions, such as Patagonia and Sahara deserts, owing a high albedo that makes them able to reflect the most of the incoming solar radiation and thus slowing down the temperature increase.

From **Figure 3.1a** and **Figure 3.1b** we can see the positive feedback mechanism involving the polar regions. When the ice melts due to temperature increase, part of the underlying land gets uncovered. Since the land's albedo is lower with respect

to the ice's one, more solar radiation is absorbed, leading to faster warming rates, which in turn accelerate the process of ice melting, creating a feedback mechanism. Due to this climate feedback, the Arctic regions warm at almost twice the rate of the global average, thus resulting in temperature increases more than doubled with respect to the global mean temperature warming. However, note that on average the Arctic amplification effect is less pronounced for models simulating a stronger AMOC weakening. This reduced temperature increase is attributed to the influence of the warming hole that arises in the North Atlantic Ocean, and spreads all around, having a cooling effect on the surrounding areas.

A peculiar spot in the North Atlantic Ocean immediately stands out when looking at **Figure 3.1b**. While the rest of the globe is expected to warm, a reversal trend affects the Atlantic ocean at high latitude with a relative SST increase significantly slower if compared to the nearby areas. Typically, this event is associated with the AMOC slowdown, which, by weakening, reduces the poleward oceanic heat transport, thus creating a minimum warming in surface air temperature immediately south of Greenland [2], which is usually referred to as the North Atlantic Warming Hole (NAWH). The effects of the NAWH is particularly intense in the Labrador Sea, Irminger sea and widely spreads from the Iceland basin towards lower latitudes. One among the investigated models (GISS-E2-1-G) even predicts an absolute temperature decrease by 2100 in that region. This cooling effect is also supposed to be amplified by other phenomena, such as the sea ice expansion allowed by the reduced heat fluxes into the Arctic region. ([2], [28]). Note also that models belonging to the large AMOC decline group show a slight warming in the equatorial Atlantic ocean, especially close to the African coasts.

This result slightly differs from the one presented in Bellomo et al. (2021), since in this study the region affected by the NAWH shows a more limited extent. The difference in SST response between the studies may have several explanations. First, in Bellomo et al. (2021), another experiment is used ($4xCO_2$), thus models are forced with different greenhouse gas concentrations in the atmosphere, increased abruptly, thus leading to different climate system responses. Furthermore, Bellomo et al. (2021) investigates climate responses over a wider time span (from year 90 to 139 of the $4xCO_2$ experiment, accounting for a total of 50 years) after AMOC's strength has stabilized, reaching a plateau for most of the simulations. My analysis is based on the last 30 years of the 21st century (from year 56 to 85), when AMOC is still declining at a sustained rate. Hence, the SST temperature response we are

analyzing is still in a transient phase, and I would expect a further evolution of its distribution, until all the simulations reach stability, thus our studies are not fully comparable. In addition to that, we should take into account the specific model's climate sensitivity. Since our samples do not account for the same models, they are characterized by different climate sensitivities, which result in different transient climate responses (TCR), thereby even analyzing the responses to an AMOC decline at the same future moment, results may differ [26]. Note that oceanic heat uptake, by delaying surface warming, affects the TCR. Thus in general, the modelization of the energy fluxes driven by the ocean plays a role in determining the climate sensitivity of a model, and as we have previously mentioned, it constitutes a major challenge and a source of uncertainty for CMIP models.

As we can see from the **Figure 3.1a**, for the models classified as small AMOC decline the NAWH is still present, but less pronounced if compared to the one predicted by the large decline scenario. The picture shows instead an enhanced warming in the subpolar North Atlantic region, being influenced by the Arctic amplification phenomenon.

Consistently with previous statements, models struggle to represent the rise of the NAWH, how it diffuses through the water column, and its connection to the AMOC decline, hence the AMOC slowdown represents a major source of uncertainty in projections of future climate change. [1] In fact, all models agree on the cooling trend above the NAWH, but its magnitude and geographical extent vary a lot across them. However, this peculiarity makes the Atlantic Ocean unique, and an extremely interesting topic in a climate change context, being the NAWH able to communicate to the overlying atmosphere and thus impacting also the global precipitation distribution and the atmospheric circulation. [29]
The NAWH has consequences on the overall temperature distribution in the Northern hemisphere, leading to a substantial widespread cooling effect. The high latitudes of the North Atlantic region are in fact known to be a climatically relevant region, playing a role in modulating the climate of north-western Europe. [30] Note that Vellinga and Wood (2008) argue that large-scale impacts may be additive. Thus, since an AMOC slowdown will occur in a warming climate, the amplitude of relative cooling in the North Atlantic and its influence on other regions' climate would depend on the magnitude and timescales of the AMOC weakening process and planet's warming trend. [2]

In conclusion, the temperature anomalies predicted by both the groups, but mainly visible in models simulating a large AMOC decline, present a warming minimum that expands from the south of Greenland to the North-western Europe. A more limited cooling seems to also involve some parts of Asia. At the same time, it is interesting to notice that North America does not experience relevant cooling. A slightly enhanced warming trend is also expected in the tropical Pacific and, albeit to a lesser extent, in the tropical Atlantic. [23]

Figure 3.1c is obtained as the difference between LAD anomalies map and SAD anomalies map, and highlights the differences between the two scenarios. It further confirms that the projected temperature anomalies are dramatically different for the sets of models. The differences are mostly pronounced in the North Atlantic ocean, in the Nordic Sea and within the deep tropics. Stippling indicates that the temperature change over North America, Greenland, North Atlantic and subpolar North Atlantic Ocean, GIN Sea, Arctic Ocean is statistically relevant, thus I argue that the AMOC decline is likely to be one of the main contributors to the creation of the NAWH, and thus drives the overall slower temperature increase predicted by the large AMOC decline scenario in the future climate change at high latitudes. The same can be said for the tropical North Atlantic Ocean. The equatorial latitudes, where heat is normally uptaken, are expected to be slightly warmer in a stronger AMOC decline scenario, although changes in surface air temperature in the tropics are generally moderate. [31] This phenomenon makes sense because in a scenario of strong AMOC decline, and thus lower levels of oceanic heat uptake, higher temperature may be expected in the Tropical Atlantic, enhancing the pace of global warming at those latitudes. [7] Also the Pacific Ocean, the Northern Indian Ocean and the equatorial Atlantic Ocean are predicted to be warmer in the LAD scenario.

I decided to further investigate the influence of the AMOC slowdown on the North Atlantic ocean temperature change by computing the R^2 regression coefficient at each gridpoint (excluding grid points over land), between the 18 model's predicted AMOC strength reductions, and the temperature change normalized by degrees of global warming (ΔGSAT). This allows us to identify a portion of the ocean whose surface temperature anomaly directly responds to the AMOC slowdown, and also estimate to which extent the SST reduction rate can be associated with the reduced AMOC's intensity. The higher is the R^2 coefficient value of a grid point, the higher is the confidence we have in saying that the reduced temperature variation, in that specific point, is linearly influenced by the AMOC's intensity reduction.

As we can see from **Figure 3.2**, the map of R^2 coefficient shows a peak in the North Atlantic ocean, in the GIN sea and below the Iceland basin. This means that in that region a lower (higher) temperature increase rate is associated with a stronger (weaker) AMOC reduction, and a good and robust linear relationship between these variables exists, depending on the specific grid point.

The R^2 coefficient presents low values in the Labrador sea and below Greenland, even if in the same region the LAD group (**Figure 3.1b**) predicts a strong cooling tendency. This can have different explanations. First, the MME performed in **Figure 3.2** takes into account all the 18 climate models, thus it makes sense that the areas do not correspond perfectly. Furthermore, although the cooling effect can be partly associated with the AMOC reduction (in fact values of R^2 are not zero), there are also other mechanisms that can drive the freshening of SST, such as the sea-ice melting. As already explained, an upper-ocean freshening in the Labrador sea inhibits water downwelling, decreases the mixed layer depth, thus weakens the deep convection, and results to be partly responsible for the AMOC decline ([29], [32]).

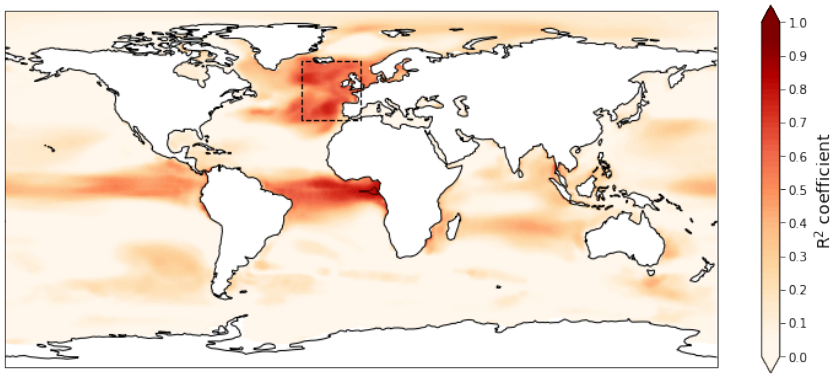

Fig. 3.2 *Map of R^2 coefficient from ensemble mean within the 18 investigated models. Black dashed box has been identified as the region in the North Atlantic basin with highest R^2 values [30°W to 0° and 35°N to 65°N].*

Note that the peak values of R^2 in **Figure 3.2** are approximately located where **Figure 3.1c** presents the stippling. Since the linear regression confirms that AMOC variability can, in large part, explain SST variability in those areas, it further confirms the goodness of the statistical tests.

I perform a linear regression, but instead of using all values, I average the SST over the black box in **Figure 3.2**. This allows us to quantify the extent to which the North Atlantic ocean's surface temperature increase rate respondes the AMOC

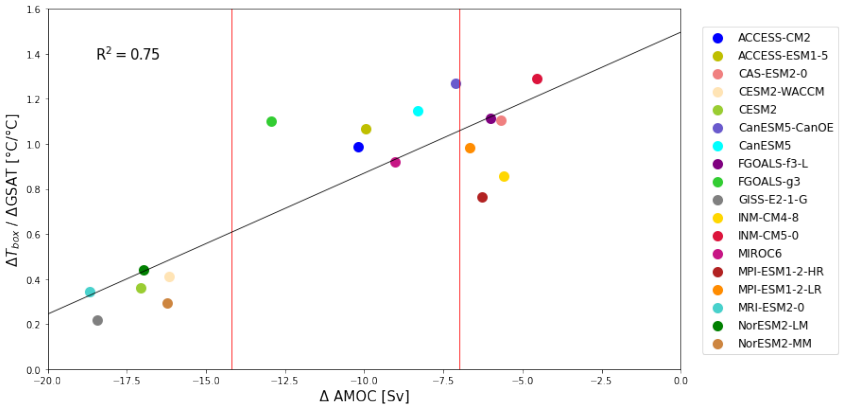

Fig. 3.3 *Linear regression between AMOC reduction and normalized SST anomaly averaged over the black dashed box. The obtained R² coefficient is around 0.71. Vertical red lines represent the terciles of the distribution.*

decline. The obtained scatter plot and relative regression line are shown in **Figure 3.3**. The R² coefficient is ~ 0.71.
The scatterplot results have two main interpretations:

- Under the same set of anthropogenic forcings, different extents of the AMOC slowdown induce different SST variations in the GIN sea.
- On average, a positive, good and robust correlation R² = 71%) exists between the AMOC reduction and SST variation.

In conclusion, the R² linear regression suggests that AMOC variation explains about 71% of the variation in upper ocean's temperature response below the Iceland basin, in the GIN sea. Note also that red vertical lines, which correspond to the terciles of the distribution, further confirm the goodness of the model's subdivision.

3.2 Precipitation anomalies and the role of AMOC in shifting the ITCZ position

Tropical Atlantic precipitation variability has been reconstructed from the last ice age, and directly observed since postindustrial period. [20] Analysis of observational data confirms the existence of a correlation between the ITCZ multidecadal fluctuations and the AMV [1]. Hence, along with a changing climate and again considering the

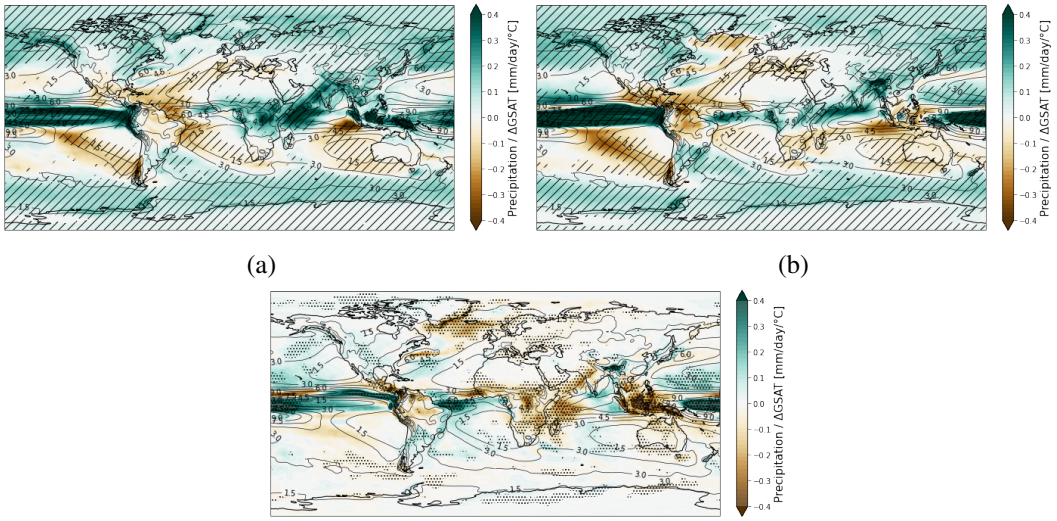

Fig. 3.4 *Precipitation anomalies for SAD group and b) in a LAD group. Superimposed black contours represent the mean climatology computed from all the 18 models. Figure c) is the difference between a) and b). The precipitation variation predicted by each models is normalized by the respective ΔGSAT, thus units of measure are mm/day per degree of global warming. Stippling indicates where the difference between LAD and SAD groups is statistically significant at the 95% threshold.*

AMOC slowdown as a sort of prolonged AMV negative phase, also the tropical rainfall variation results in some recognizable large-scale patterns.

AMOC strongly influences the North Atlantic sea surface temperature by transporting a massive amount of heat poleward, that is then progressively released to the atmosphere. As we saw in the previous section, a declining AMOC would lead to a reduction of available heat over the NA ocean, and thus a strong cooling effect. Surface temperature variation is a driving element for changes in evapotranspiration, which in turn regulates the amount of water in the atmosphere, and thus the intensity of rainfall events. At the same time, atmospheric circulation drives the rainfall spatial distribution and intensity amongst the Earth's system, being influenced by AMOC and in turn influencing AMOC itself. Hence, there are several mechanisms that can be considered drivers of precipitation changes. In this section I will analyze the impacts of the AMOC on the mean annual precipitation changes, whereas a deeper analysis of the driving mechanisms of such changes will be performed in the next section.

Figure 3.4a and **Figure 3.4b** show the changes in precipitation for the two sets of models. Here I evaluate inter-model reliability to assess whether there is inter-model agreement in the precipitation changes with respect to the historical run. Hatches indicate where all the models belonging to each group agree in sign for each point of the grid.

For both groups of models, the largest positive changes occur in the deep tropics, mainly in the equatorial Pacific. There are positive changes also at very high latitudes of both hemispheres, with a good inter-model agreement. On the other hand, the largest reduction in precipitation is expected to occur above the North-East region of South America and central America, especially over Brazil, Guatemala, Mexico, and the Amazon region [4]. However, there is no inter-model agreement about the intensity and localization of such precipitation changes [2], especially over the inland regions. The same can be said also for Southern and Northern inland Africa, Southern Europe, Western Asia and most of the Australian continent, where changes in precipitation are generally predicted to be small. Note that in general the already arid or semi-arid regions (such as the subtropical dry zones) undergo a further drying tendency. All these regions where a precipitation reduction is expected to occur are very likely to be subjected in future to even higher water resources stresses. Whereas a small AMOC decline scenario generally predicts a strengthening of the hydrological cycle, under a large decline the precipitation variation deviates from this behavior, showing a drying tendency in the Gulf stream and over the region insterested by the NAWH. Models simulating a stronger decline agree on the precipitation reduction over the higher latitudes of NA ocean, caused by the temperature cooling (NAWH). In a small decline scenario instead there is no common agreement on the precipitation change sign. This derives from the fact that some models of the SAD group predict a poor cooling effect, thus a precipitation reduction, whereas in some other models the cooling effect is absent and temperature slightly warms, thus inducing a precipitation increase.

The differences in rainfall distribution expected for the two sets of models **Figure 3.4c** present some interesting features. At very high latitudes, differences between the two groups are small. Larger differences appear while moving through the equator. Specifically, Central and South Africa, Australia, Philippines ocean and part of the western Indian Ocean are predicted to be drier by the large AMOC decline groups, with respect to the small AMOC decline group. Proper tests confirm the statistical relevance of these differences. The same can be said for part of Europe, Western

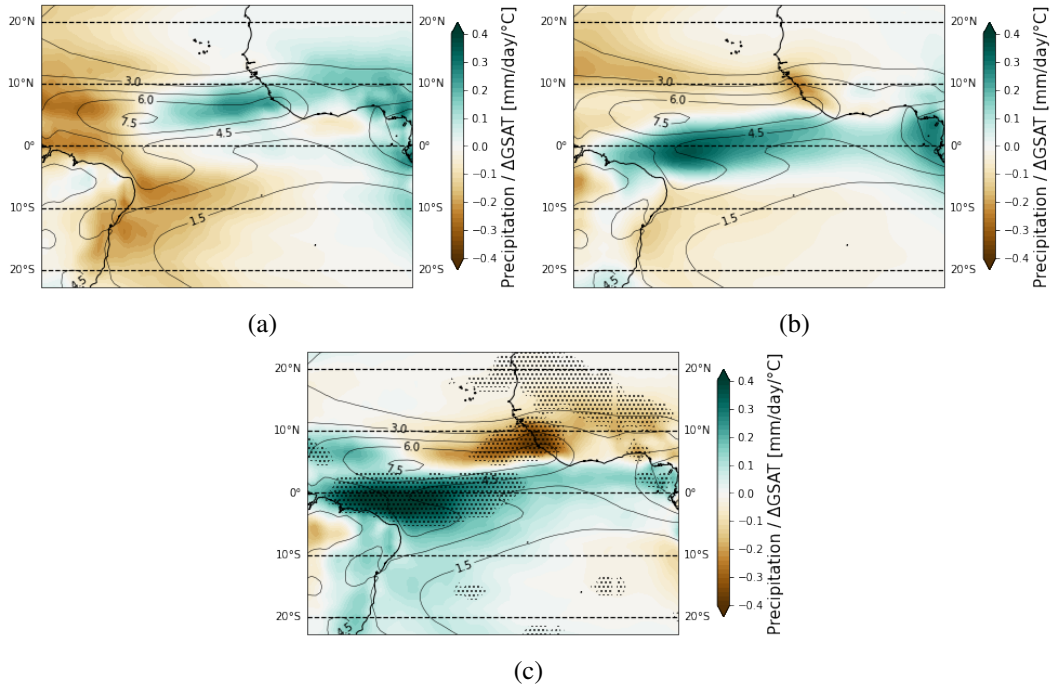

Fig. 3.5 *Zoom in on the tropical Atlantic band. a) Precipitation anomalies for SAD group and b) in a LAD group. Superimposed black contours represent the mean climatology computed from all the 18 models. Figure c) is the difference between a) and b). The precipitation variation predicted by each models is normalized by the respective ΔGSAT, thus units of measure are mm/day per degree of global warming. Stippling indicates where the difference between LAD and SAD groups is statistically significant at the 95% threshold.*

Asia, the Gulf stream and the NAWH. Also, a large portion of the Mediterranean Sea is expected to get drier if a large AMOC decline occurred. At the same time, an opposite trend would be expected in Southern America and the tropical Pacific ocean. Note that rainfall changes induced by a weakened AMOC are particularly intense and statistically relevant in the equatorial zonal band spacing between Brazilian coasts and the African continent, where precipitation anomalies flip their sign between the two Hemisphere, around the equatorial latitude.

The AMOC impacts also involve the Indian monsoons. Despite all the models of both the groups predict an increase in rainfall intensity (confirmed by the inter-model reliability analysis), **Figure 3.5c** indicates that in a LAD scenario the precipitation increase is lower if compared to the SAD scenario, suggesting that India may experience more frequent droughts if a strong AMOC decline occurred. Previous studies have pointed out that an AMOC slowdown may interfere with the Asian monsoon by modifying the interhemispheric temperature gradient, thus shifting the

mean annual position of ITCZ, and affecting the strength of westerly winds that usually interact with the southerly monsoon winds (see **Appendix F**). [9]

Focusing our attention on the Atlantic Ocean where changes are large and statistically significant, we see that the large AMOC decline group shows a dipole pattern of precipitation (**Figure 3.5b**). [4] Whereas negative anomalies are detected over the tropical and subtropical North Atlantic Ocean and over the GIN sea, positive anomalies are expected over a narrow equatorial belt, spacing between the western American coast and the Eastern African coast. The negative anomalies can reasonably be induced by the reduced warming caused by the rising of the NAWH, that in turn causes a reduction of surface water evaporation and consequently a reduction of precipitation. At the same time, the positive anomaly detected over the equator cannot be explained so easily. However, it is a first clue suggesting that models belonging to the large AMOC decline group show an equatorward shift of the tropical precipitation band (the ITCZ), which in fact does not appear in the small AMOC decline precipitation anomalies map. In contrast, **Figure 3.5a** shows a strong positive variation in a region just above the equator, with limited meridional extent. All around there are instead negative changes. **Figure 3.5c** highlights the strongly different behavior of the two groups of models, highlighting that under a large AMOC decline the equator would be largely wetter, while slightly higher latitudes would be largely drier if compared to a small decline scenario. The tests confirm the statistical relevance of differences between the two groups' climate responses over the tropical Atlantic area, allowing us to argue that the AMOC slowdown is a major cause.

To strengthen the analysis about predicted tropical Atlantic precipitation changes, I perform a further step by examining the anomalies of the annual zonal mean precipitation for the two sets of models, averaging values over a range of longitudes corresponding to the tropical Atlantic Ocean (40W-20E). Results are reported in **Figure 3.6**. The black curve represents the zonal mean climatology of precipitation over the Atlantic Ocean. The ITCZ is visible as the peak of precipitation occurring around 5°N, thus confirming its northward position as a response to cross-equatorial atmospheric energy fluxes, as hypothesized by Marshall et al. 2014 and Frierson et al. 2013. The red and blue curves represent the zonal mean precipitation anomalies predicted by the two sets of models.

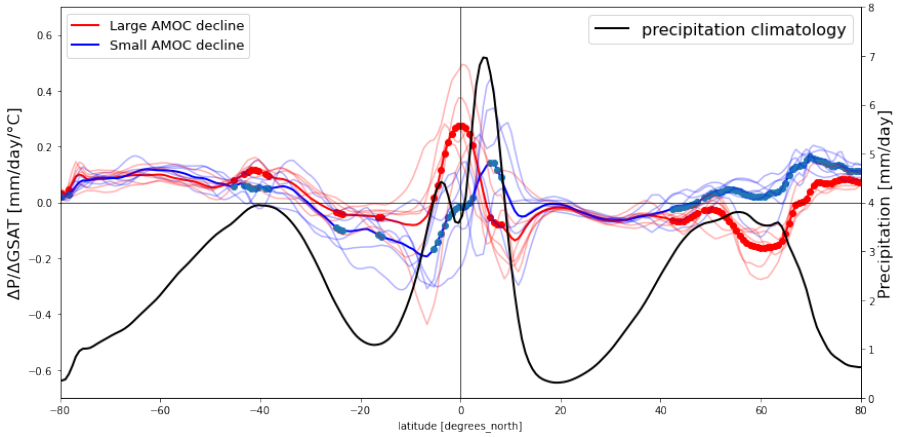

Fig. 3.6 *Black curve is the zonal mean precipitation climatology averaged on the longitudes corresponding to the North Atlantic computed from the historical run of all the 18 models, and refers to the right axis. Blue (red) curve represents SAD (LAD) zonal anomalies and refers to the left axis. Lighter blue (red) lines are the zonal mean precipitation variation predicted by each of the models belonging to the SAD (LAD) group. Round markers indicate where the difference is statistically significant at the 95% threshold.*

The blue curve (zonal anomalies in SAD scenario) exhibits a positive anomaly around 5°N, so the aforementioned asymmetry is expected to intensify. The red curve (zonal anomalies in LAD scenario) instead, shows a positive peak shifted towards the Equator, while it's negative around 5°N and northward in the tropics. Thus the zonal distribution of precipitation is going to change along with a strong AMOC decline. The consequent reduced meridional heat transport, reducing the inter-hemispheric asymmetry in rainfall distribution, tends to move the ITCZ towards the equator. This zonal displacement is absent in the precipitation anomalies predicted by the small decline group.

In general terms, over the tropical Atlantic ocean the set of models simulating a weaker decline follows quite well the "dry-get-drier, wet-get-wetter paradigm" that is, areas which already have an excess of precipitation over evaporation of the deep tropics and mid-latitudes will get wetter and arid and semiarid regions in the subtropics will get drier [33]. In contrast, the LAD group does not follow the paradigm and shows a more complex behavior. Previous analysis suggests that the ITCZ southward displacement is closely tied to changes in atmospheric energetics and reduced eddy moisture transport [23]. Such precipitation anomalies arising under a large AMOC decline scenario may have huge impacts for the local climate, with

large consequences on the hydrological cycle of many regions, mainly pronounced in the Amazon region and Africa [2].

The plot in **Figure 3.6** focuses on the longitudes corresponding to the North Atlantic sector, but still confirms that major changes occur in the tropics and at those latitudes interested by the NAWH rising, where the differences are also statistically relevant, as suggested by the round markers on the curves. At very high latitudes in the Southern Hemisphere (Antarctica) no relevant differences between the two groups can be detected. I note some rainfall differences at the Southern subtropics level, but the sign of the variation remains coherent between the two groups. The two curves have strongly opposite signs, and thus completely opposite responses, at NAWH latitudes, with the large AMOC decline group predicting a drying tendency (lower temperature and consequently lower evaporation) and small decline group predicting a wetting tendency by the end of the century. This is a direct consequence of changes in evaporation.

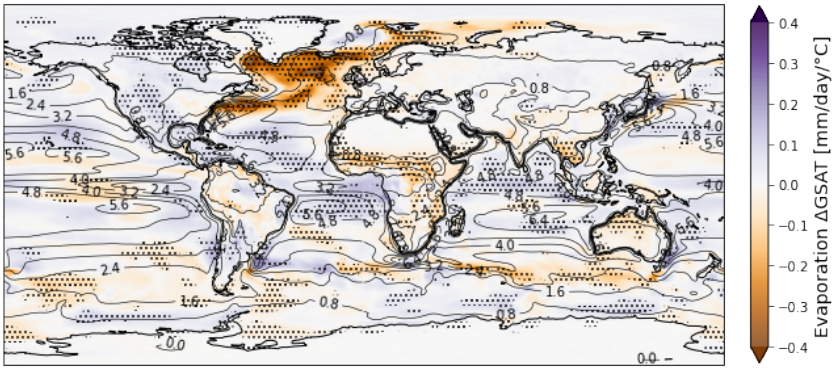

Fig. 3.7 *Evaporation difference between anomalies predicted by the LAD group and anomalies predicted by the SAD group. The evaporation variation predicted by each models is normalized by the respective ΔGSAT, thus units of measure are mm/day per degree of global warming. Stippling indicates where the difference is statistically significant at the 95% threshold.*

Single anomalies maps for the evaporation for the two sets of models are shown in **Appendix E**.

The evaporation phenomenon over all the North Atlantic basin is expected to reduce in response to a weaker AMOC strength as less water evaporates from the ocean to the atmosphere, as a consequence of the reduced temperature warming [23]. In contrast, an overall increase of evaporation rate is expected for the rest of the planet. This phenomenon can be explained by the Clausius-Clapeyron relationship

[19], according to which an increase in surface temperature would cause an increase in the quantity of water vapor retained by the atmosphere. Thus, evaporation changes mirror quite faithfully the global pattern of temperature change [28].

Focusing only on the North Atlantic sector, given the temperature reduction caused by a strong AMOC decline, what we could expect is an overall reduction of precipitation, caused by the reduced water vapor into the atmosphere (reduced evaporation). However, as the precipitation pattern of change shows a more complicated configuration, it is worth it to explore this particular behavior in more detail. In **Section 4**, by performing an atmospheric moisture budget, I associate these differences in tropical precipitation anomalies between the two groups to the relative influence of thermodynamic and dynamic drivers of precipitation changes.

3.3 The response of the Hadley circulation and linkage with the ITCZ

After assessing the ITCZ southward shift predicted by the models simulating a large AMOC decline, in this section I analyze the Hadley circulation anomalies, highlighting the linkage with the Atlantic tropical precipitation pattern of change.

The global distribution of precipitation is largely shaped by the atmospheric Hadley circulation, which is responsible for energy and moisture transport from the equatorial latitudes to the subtropics. In particular, the upper branch of the SH (NH) cell transports energy towards the Southern (Northern) Hemisphere, pushing warm air into the descending branch. While moving down, air warms adiabatically by compression from the overlying atmosphere, and creates a zone of high pressure. Thus, air is pushed equatorwards, back to the low-pressure ascending branch of the cell, absorbing moisture along the way. Where the lower branches of the two Hadley cells converge, moistened air rises, producing intense convective rainfall events.

Since the ITCZ is located in the ascending branches of the cells, evidence of its displacement highlighted in **Section 3.2** may suggest a coherent modification of the Hadley cells. In fact, as a consequence of an AMOC decline, less oceanic heat would be uptaken in the SH and transported northward, thus reducing the need for the compensating mechanism acted by th e cross-equatorial SH Hadley cell, which in a usual condition has the aim of minimizing the energy transport

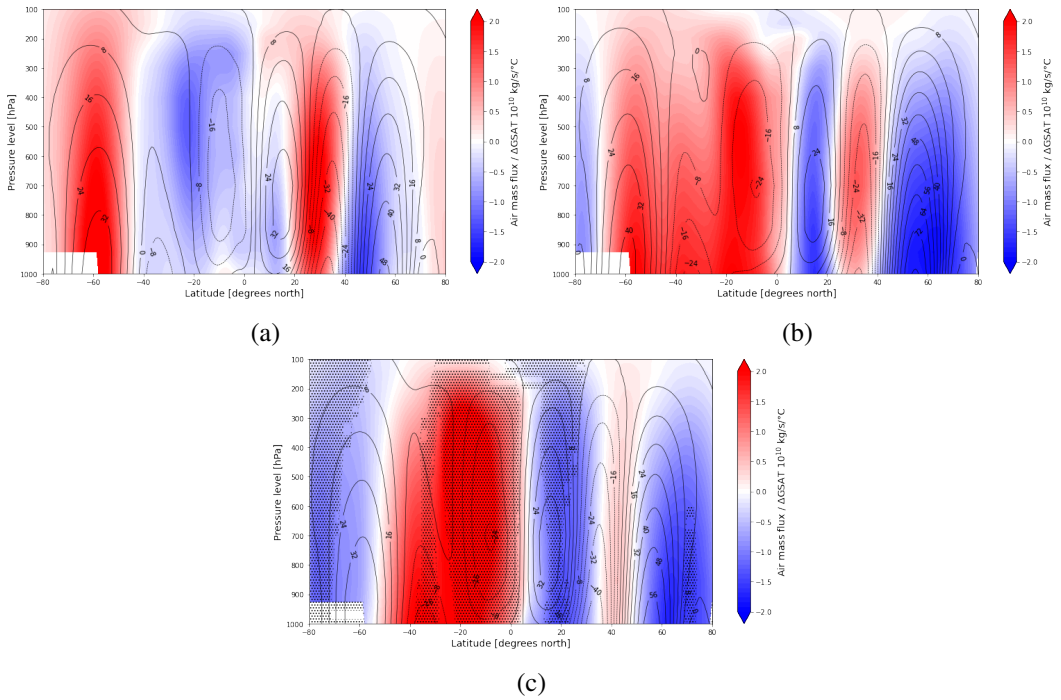

Fig. 3.8 *Mean annual tropical Atlantic Hadley circulation anomalies for a) SAD group and b) LAD group. Superimposed black contours represent the mean annual climatology, one is computed for each set of models. Negative values indicate an anti-clockwise circulation, while positive values correspond to a clockwise one. Figure c) is the difference between a) and b). The atmospheric circulation variation predicted by each models is normalized by the respective ΔGSAT, thus units of measure are* $10^{10}\ \frac{kg}{s}$ *per degree of global warming. Stippling indicates where the difference is statistically significant at the 90% threshold.*

imbalance between the Hemispheres [20]. Several previous studies, such as Zhang and Delworth (2005), have already proven that the mean annual position of the ascending branch of the Hadley cells becomes more symmetric about the equator under a simulated substantial weakening of the Atlantic thermohaline circulation.

According to Zhang and Delworth (2005) and my results too, the tropical Pacific atmospheric circulation responses to an AMOC slowdown are much smaller than those detectable over the Atlantic Ocean. Thus, to have a clearer signal, here I show the atmospheric circulation response to an AMOC decline over the tropical Atlantic latitudes.

Black contour lines represent the annual mean climatology for both the sets of models. In the coordinates used for this plot, the climatology of the mean annual Hadley circulation is characterized by a clockwise rotation in the Northern

Hemisphere (here represented by positive values) and an anti-clockwise rotation in the Southern Hemisphere (negative values). Note that the climatology of both the models reveals a smaller NH cell and a more expanded SH cell, crossing the Equator, thus transporting more heat southward than northward. Figures also show the annual bulk northward shift of the cells, localizing the ascending branch of the Hadley cells at about 5°N, and thus further confirming the climatological mean annual positioning of the ITCZ already found in the previous section.

In a future scenario where AMOC is projected to decline, thus reducing the oceanic energy transport that drives the mean annual Hadley circulation displacement, some modification for the actual Hadley circulation is expected. In a weaker AMOC decline configuration (**Figure 3.8a**), the blue area that spreads between 5°N 40°S suggests that the mean annual SH cell strengthens its intensity, especially around 20°S, and clearly shows a poleward expansion tendency. The NH cell instead weakens at lower latitudes (blue area in the lowest levels of the atmosphere between 5°N and 18°N) and expands towards higher latitudes (red area between 20°N and 40°N). The mid-latitude cells in both the Hemispheres are compressed by the Hadley cells expansion, and presumably pushed poleward. Both the Hadley cells are thus expected to expand under a small AMOC decline scenario, with consequent poleward shift of the dry descending branch. [34]

This widening phenomenon, which has already been confirmed by recent studies and direct observations [12], is of particular interest in a context of climate change. There is some observational evidence according to which in the last 40 years the Hadley cells have expanded at a rate of about 0.1°–0.5° latitude per decade, raising concern about the possible poleward displacement of the subtropical dry zones. The driest regions on Earth, such as the subtropical dry zones and many desertic areas, are in fact localized under the dry descending branch of the Hadley cells. Here, air begins traveling in the lower branch of the cell, fluxing away moisture and bringing it into the moist deep tropics. Even a small change in the HC meridional extent, and thus a poleward displacement of the descending branch, would cause a coherent poleward displacement of the dry zones, causing water resource stress in many regions. [14]

When models simulate a larger AMOC decline (**Figure 3.8b**), a largely different response is seen. The red area between 0 and 5°N suggests a weakening of the mean annual SH cell (that further spreads towards lower latitudes). It may also

be interpreted as an equatorward shift of the NH cell. Note that these results are analogous to those highlighted by analyzing **Figure 3.6**. In the NH not only the Hadley cell weakens, but also the mid and high-latitude cells appear to rotate with less intensity.

The circulation intensity weakening of both the cells occurring under a large AMOC decline scenario is dramatically different from the (weak) strengthening expected in a small AMOC decline scenario, as suggested by the central red and blue areas in **Figure 3.8c**. Stippling between 20°N and 40°S confirms that the AMOC decline can be considered the main driver of this weakening effect, that around 5°N can also suggest a bulk southward shift of the cells. There is poor confidence in attributing the cells weakening at higher latitudes to the AMOC decline. However, many studies suggest that the HC slowdown and widening is consistent with the enhancement of atmospheric stability caused by a warming climate, hence it makes sense that the AMOC decline does not have to be considered the driving mechanism of these phenomena at high latitudes. [34]

The strengthening of the mean annual SH cell in the SAD future projections can be confusing, and deviates from the direct observations' evidence that instead indicate that the cells have undergone a period of decline. This may be due to the fact that the atmospheric circulation varies seasonally, and large spatial shifts occur during the year. Hence, a better understanding can be achieved from the analysis of the seasonal Hadley Cell. As we will see, since the atmospheric circulation varies cyclically, the seasonal response of the Hadley cell to an AMOC decline differs from the mean annual anomaly, because of the dominance of the winter cell in the boreal and austral winter seasons. A stronger rotation intensity characterizes the wintertime cells than the summer cells. [31]

I focus on the two main seasons JJA (June - July- August, austral winter) and DJF (December-January-February, boreal winter). Roughly speaking, both seasons show some common features already explained for the mean annual HC, and some common deviations from it. For the sake of simplicity, only figures related to JJA are shown here and commented on. Analysis of DJF can be consulted in **Appendix E**.

In JJA, the small AMOC decline group shows a weakening trend for both the cells around the equator, with anomalies whose sign is opposite to the climatological rotational direction of the wind. This weakening is not visible when analyzing the mean annual atmospheric circulation over the NA. However, since a slowdown of the

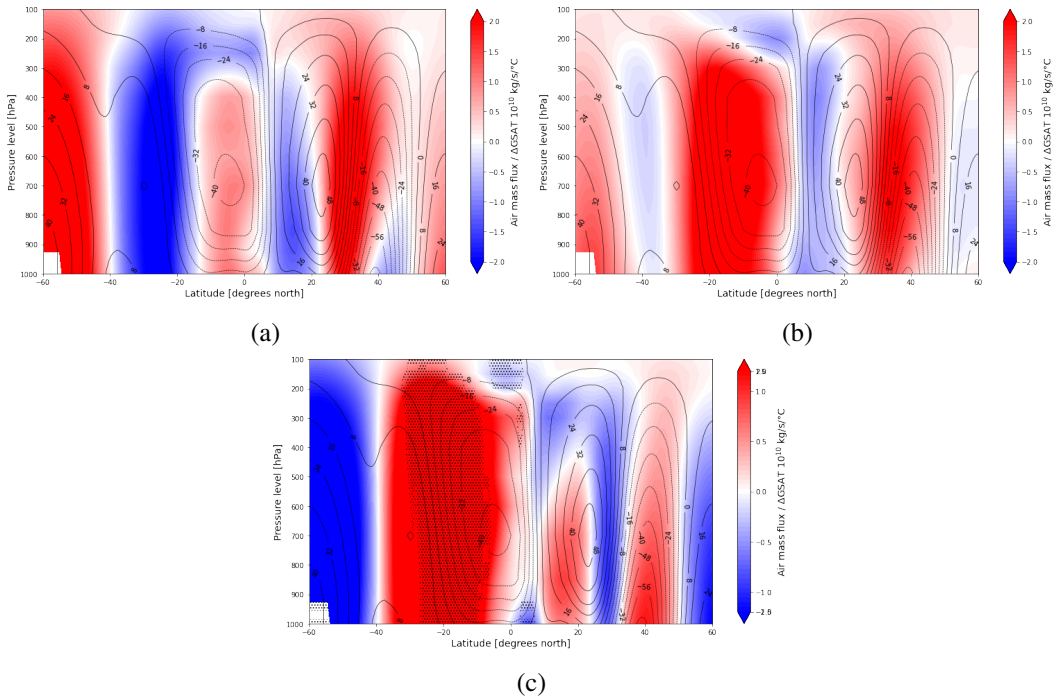

Fig. 3.9 *Tropical Atlantic Hadley circulation anomalies in boreal winter season (JJA) in a) SAD scenario and b) LAD scenario. Panel c) is the difference between the two. Superimposed black contours represent the mean seasonal climatology. Negative values indicate an anti-clockwise circulation, while positive values correspond to a clockwise one. The atmospheric circulation variation predicted by each models is normalized by the respective ΔGSAT, thus units of measure are* $10^{10}\ \frac{kg}{s}$ *per degree of global warming. Stippling indicates where the difference is statistically significant at the 90% threshold Stippling indicates where the difference is statistically significant at the 90% threshold.*

Hadley Cells derives from an enhanced atmospheric stability caused by a warming climate, a weakening trend (more or less pronounced) can be expected for all the seasons. For both the NH and SH cells a strong meridional expansion tendency is visible, causing also a weakening and compression of the mid-latitudes cells. As mentioned before, this is a typical trend that has already been recorded by direct measurements and can be attributed to the reduction of temperature gradient between the equator and higher latitudes, due to the warming climate.

For the large AMOC decline group, anomalies show a more complex behavior. Whereas the NH cell weakens at low latitudes and expands towards higher latitudes, the SH cell (thus the dominant one in austral winter) instead of expanding, undergoes a strong intensity reduction that spreads from the equator towards lower latitudes. Statistical tests reveal that the SH cell's intensity reduction in the LAD group is

driven by the AMOC decline, that by declining reduces the need for a compensating southward energy transport, thus reducing the need for a cross-equatorial SH cell. According to **Figure 3.9c**, the simulated NH cell intensity reduction is stronger in future projections of models belonging to the LAD group. However, there is no high confidence in saying that it could be a direct consequence of the AMOC decline. Furthermore, what emerges is that the expansion tendency of the NH cell under a strong AMOC decline scenario is limited, in contrast to the enlarged cells observed in a warming climate. Even if one possible reason could be the increased equator-to-pole temperature gradient due to the reduced heat transport by the oceanic currents, statistical tests do not allow us to consider the AMOC decline as the main driver of this behavior.

Chapter 4

Moisture budget

As examined in the previous section, tropical Atlantic precipitation patterns of change predicted by the end of the 21^{st} century by the two sets of models show different behaviors, and rigorous statistical tests confirm AMOC's decline as a major driver of their differences.

Many studies have already proven that a warming climate causes an increase of the amount of water vapor into the atmosphere, as also expected simply from the Clausius-Clapeyron equation. Thus, if the atmospheric circulation remained unchanged, we would be expect an intensification of the current pattern of precipitation due to thermodynamic constraints, thus leading to the "wet get wetter - dry get drier" mechanism, which is in agreement with the behavior of the small AMOC decline future projections of precipitation over the tropical Atlantic ocean [35]. However, it is clear that this thermodynamic mechanism alone is not sufficient to explain the variation in the tropical Atlantic precipitation spatial distribution occurring under a large AMOC decline scenario. In the LAD future simulations the ITCZ shows a southward shift, thus a prevailing dynamical contribution linked to changes in the atmospheric circulation changes may be expected for this group of models. In fact, as previously observed in **Section 3.3**, the zonal Hadley circulation is projected to undergo major changes with time. In turn, according to a study conducted by Trenberth and Guillemot (1995), the moisture transport within the tropics is very dependent on the divergent component of the wind field.

Changes in the hydrological cycle may have important implications for human societies and ecosystems, thus it is worth understanding the dominant processes

that govern the net precipitation differences between the two AMOC groups. In this section, following the procedure introduced by Seager et al. (2010), I analyze the main contributors to changes in moisture into the atmosphere, that lead to the precipitation changes.

4.1 Methodology

To better understand the underlying mechanisms involved in net precipitation (precipitation minus evaporation, P-E) changes, Seager et al. (2010) suggests performing a moisture budget, thus reconstructing with physically-based equations the amount of precipitable water available into the atmosphere, the precipitation minus evaporation, computed as a residual from the large-scale atmospheric transport. The moisture budget equation derives from a combination of the equation of state, the hydrostatic equation, and the continuity equation. [36]

As a result, the moisture budget equation that I use the following:

$$\rho_w g(P-E) = \int_0^{p_s}(\bar{u}\cdot\nabla\bar{q}+\bar{q}\cdot\nabla\bar{u})dp - \int_0^{p_s}\nabla\cdot(\overline{u'q'})dp - q_s u_s\cdot\nabla p_s$$

where the overbars indicate monthly means and primes indicate deviations from the monthly mean (for instance u = u + u'). The datasets involved to complete the moisture budget are: surface pressure (p), specific humidity (q), zonal wind vector (u), meridional wind vector (v). The subscript "s" is related to surface values. ρ_w is the density of water.
The equation is then discretized and solved at each grid point, for all the models under investigation. The vertical integration is performed over the 17 higher pressure levels (the 17 levels closest to the Earth's surface, between 1000 hPa and 10 hPa), and allows us to quantify the total amount of water contained from the bottom to the top of the atmosphere.

The first integral describes the moisture transported by the mean flow, given by the vertically integrated divergence of the atmospheric moisture flux ($q\cdot u$). It will be splitted in a thermodynamic term and a dynamic one, represented by the two addenda into the integral. These terms will be further decomposed in a divergent term and an advective one (spatial gradients of q and u are performed using finite differences). The second integral contains the horizonal velocity and specifitc humidity deviations

from the time mean (turbulent moisture flux), and thus represents the transient eddies. The last term contains information related to surface quantities, which are related to moisture transport deformations due to surface pressure gradients (mainly caused by the orography). [37]

The differences between variables evaluated in the two saved periods (20^{th} and 21^{st} centuries) are used to describe inter-century variations, with the following notation:

$$\delta(\cdot) = \delta(\cdot)_{21} - \delta(\cdot)_{20}$$

Thus we can rewrite and approximate the first equation as follows:

$$\rho_w g \delta(P-E) \approx$$
$$-\int_0^{p_s}(\delta\bar{u}\cdot\bar{q}_{20} + \bar{u}_{20}\cdot\nabla\delta\bar{q} + \delta\bar{q}\nabla\cdot\bar{u}_{20} + \bar{q}_{20}\nabla\cdot\delta\bar{u})dp - \int_0^{p_s}\nabla\cdot\delta(\overline{u'q'})dp - \delta S$$

The linear decomposition of the last equation results in the four components of our interest [33], each one representing a different mechanism that can cause a precipitable water availability spatial change.

- The term involving changes in mean specific humidity is classified as the thermodynamic contributor:

$$\delta TH = \int_0^{p_s}\nabla\cdot(\bar{u}_{20}[\delta\bar{q}])dp$$

- The term involving changes in the mean horizontal velocity is classified as the dynamic contributor:

$$\delta DY = \int_0^{p_s}\nabla\cdot([\delta\bar{u}]\bar{q}_{20})dp$$

- The term containing specific humidity and horizontal wind speed fluctuations with respect to the mean values describes changes related to the transient eddies:

$$\delta TE = -\int_0^{p_s}\nabla\cdot\delta(\overline{u'q'})dp$$

- The surface quantities term is estimated as a residual.

The synthetized equation is the following:

$$\rho_w g \delta(P-E) = \delta TH + \delta DY + \delta TE + \delta S$$

The moisture budget calculations are separately performed for each model, supplying as an output the contribution of each term for each model.

To evaluate the goodness of the results, the terms are summed according to the equation above (phase of reconstruction of net precipitation through moisture budget) and compared to the relative net precipitation predicted by the available datasets: precipitation (pr) minus evaporation (evspsbl). For each model under investigation, the differences between the two are small and absolutely negligible, confirming the correctness of the calculations. Only one exception is related to the GISS-E2-1-G model, whose dataset is corrupted, thus it has been excluded from this analysis.

Finally, MMEs amongst the members of the two groups are performed, to visually and quantitatively evaluate the relative contribution of each term to the moisture budget, for the two scenarios under analysis.

4.2 Results

The following maps represent the net precipitation, thus show residuals of precipitation minus evaporation maps (P - E) that have been reproduced with the moisture budget. As expected, the maps show lower values at mid-latitudes with respect to precipitation maps in **Section 3.2**, being part of the water subjected to evaporation, that is projected to increase worldwide as a consequence of increasing temperatures (see **Appendix E**). The region interested by the rise of the NAWH constitutes the only large and notable exception. The anomalies sign flips with respect to the sign predicted if only precipitation changes were taken into account, revealing strongly positive anomalies of precipitable water also for the large AMOC decline simulations.

There is no common agreement among the models about which term of the moisture budget provides the largest contribution to the P-E budget, also the intensity of the related anomalies is uncertain, and the spatial structure of patterns of changes shows a high variability and dishomogeneity. [38] The reason for this high spatial variability is the transport of the water vapor operated by the mean and time-varying flow into the atmosphere [33]. As a general rule, evaporation exceeds precipitation

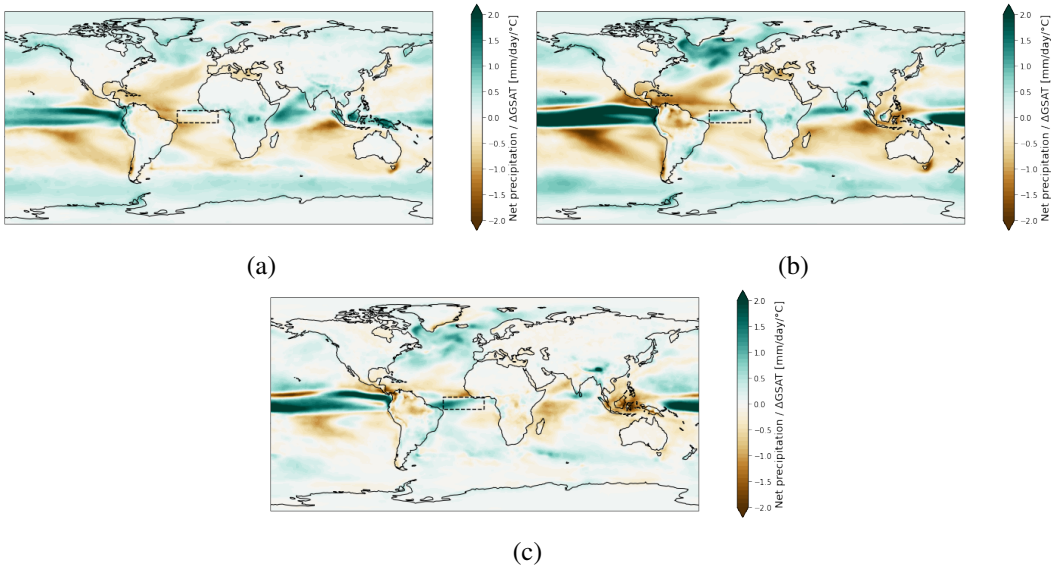

Fig. 4.1 *Net precipitation anomalies for a) SAD group and b) in a LAD group. c) is the difference between a) and b). The black box corresponds to the coordinates [35W -0W - 4S - 6N], and will be used in* ***Section 4.2.4****. The net precipitation variation predicted by each models is normalized by the respective ΔGSAT, thus units of measure are mm/day per degree of global warming.*

over oceanic areas, leading to drier climate within the subtropics. At the same time, precipitation over inland regions exceeds evaporation, thus leading to positive residuals of P - E on average. [36] However, a detailed global analysis is unfeasible for this work.

However, focusing our attention on the tropical Atlantic Ocean, some peculiarities are evident, that are analogous to those observed in **Section 3.2**. The group of models simulating a weaker AMOC decline show a drying signal widespread above both the Hemispheres, that intensifies close to the Central American coasts. Small positive changes are localized at a latitude of 5°N, in correspondence to the mean annual position of the ITCZ, following the "wet-get-wetter" paradigm. Models simulating a stronger decline instead predict a weaker drying signal for both the Hemispheres. In addition to that, a narrow positive band is localized at the equator, suggesting that the ITCZ has been displaced equatorwards. **Figure 4.1c** highlights these differences: if a large decline occurred, climate would appear to be much wetter at the equator and drier just above it, corroborating the hypothesis.

In the next sections, maps are zoomed in on the tropical Atlantic region. The global pictures can be found in **Appenidx F**.

4.2.1 Moisture budget: the thermodynamic contribution

As already mentioned, the thermodynamic contributor deals with variations in the vertically integrated mean specific humidity, thus it is at least in part constrained by the Clausius Clapeyron relationship, and so by the ongoing global warming. It is not surprising to notice that the anomalies owed to thermodynamic drivers (**Figure 4.2**) have quite the same spatial pattern for the two sets of models, especially between 2°N and 9°N, near the South American coast, with a clear positive signal, but appear to be more intense under a large AMOC decline scenario. This happens because the thermodynamic changes in large part follow the increase in specific humidity, deriving from an atmosphere that in a large AMOC decline scenario is expected to be warmer at equatorial latitudes. This relative warming has already been pointed out and described in **Section 3.1**.

As a result, the map of differences between large and small AMOC declines has quite the same pattern predicted by the large decline group, indicating that the two anomaly maps mainly differ in terms of absolute values and variations are stronger in a strong decline scenario. It is the pathway that would be followed by the precipitation distribution under the current global warming if absolutely no dynamic changes in the planet's atmosphere were to occur.

Thus, the thermodynamic term still does not tell us anything relevant about the peculiar pattern of net precipitation changes that we noticed as a response to a large AMOC decline.

Note that since both in **Section 3.2** and in **Figure 4.1a** we observe the "dry-get-drier, wet-get-wetter" behavior for the SAD group, it is very likely that the thermodynamic drivers of net precipitation change are the dominant contributions to net precipitation changes if a small AMOC decline occurred.

4.2.2 Moisture budget: the dynamic contribution

As we can see from **Figures 4.3a and 4.3b**, the dynamic contributor to net precipitation change clearly shows differences in the spatial distribution over the tropical Atlantic region for the two sets of models.

Under a simulated small AMOC decline, a drying tendency prevails at the equatorial latitude and beyond, spreading in both the Hemispheres. It is mainly

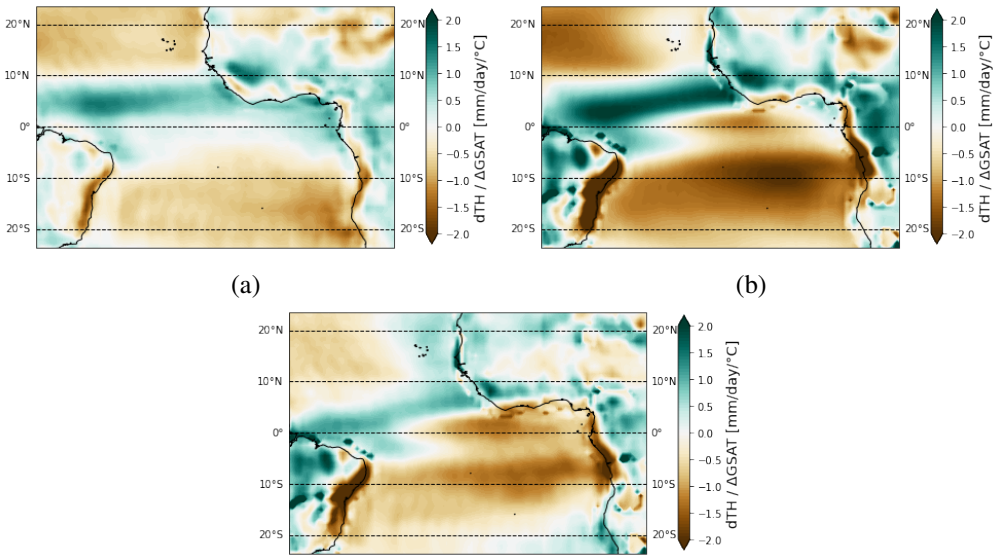

Fig. 4.2 *Thermodynamic contribution to the moisture budget changes for a) SAD group and b) in a LAD group. c) is the difference between a) and b). The thermodynamic contribution predicted by each models is normalized by the respective ΔGSAT, thus units of measure are mm/day per degree of global warming.*

pronounced close to the Central American coasts, in agreement with **Figure 4.1a**, thereby probably prevailing on the thermodynamic term in this specific area. Despite the overall drying, a small oceanic region close to the African coast shows a slightly positive variation.

On the other hand, under a large AMOC decline scenario, the spatial pattern of moisture distribution change reveals an extremely clear band with positive sign between the equator and 2°N (more or less in the same position where the thermodynamic contribution assumes a negative sign), and a strong drying tendency just above this latitude. This is the same behavior predicted by the zonal mean precipitation changes examined in **Section 3.2**, and further confirmed by similarities with **Figure 4.1b**, with negative changes predicted at 5°N and positive changes at the equator. Thereby, we can come up with two observations:

1. This dynamic term should be strong, and prevailing on the thermodynamic contributor in a LAD scenario.

2. Since **Figure 4.3b** presents positive anomalies at the equator, and negative anomalies slightly above it, we can recognize the pattern of change that

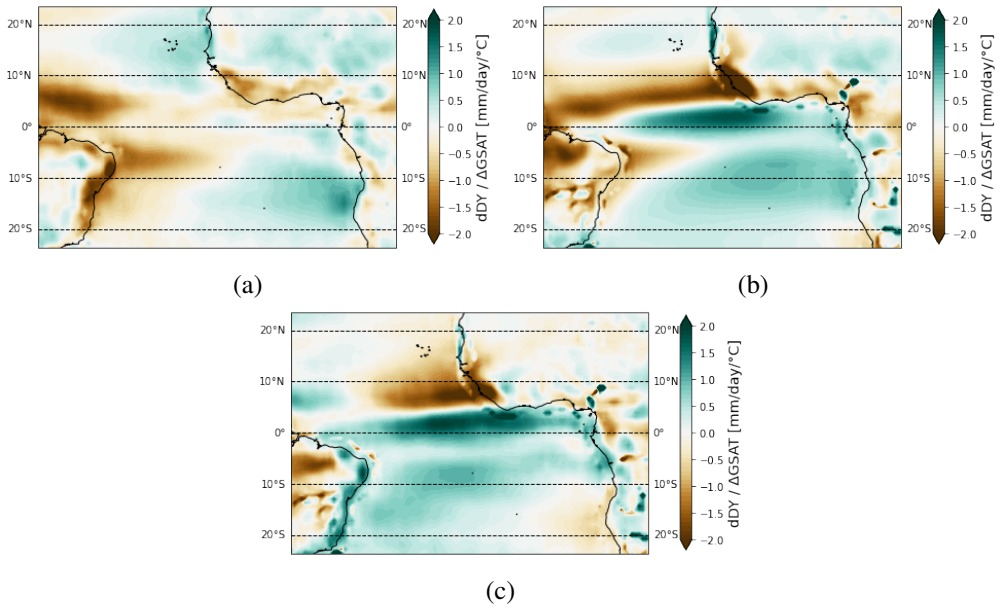

Fig. 4.3 *Dynamic contribution to the moisture budget changes for a) SAD group and b) in a LAD group. c) is the difference between a) and b). The dynamic contribution predicted by each models is normalized by the respective ΔGSAT, thus units of measure are mm/day per degree of global warming.*

suggests an ITCZ displacement. Thus, to this dynamic term we can attribute the merit of pushing the ITCZ southward, driven by large-scale Hadley circulation changes, that in turn cause surface wind anomalies with respect to the mean annual horizontal wind field within the tropics.

Thus, as a response to a strong AMOC decline, the equator is projected to be dynamically moistened, while the reversal effect occurs at slightly higher latitudes, which are instead dynamically dried. Note that for the large AMOC decline group the dynamic contributor at the equator has an opposite sign with respect to the thermodynamic one, but it is strong enough to dominate over it and drive the predicted moistening. Thus, wind-driven variations in the tropical atmospheric circulation caused by a strong AMOC slowdown somehow offset and overcome the changes induced by the warming atmosphere [33], dominating the precipitable water patterns of change.

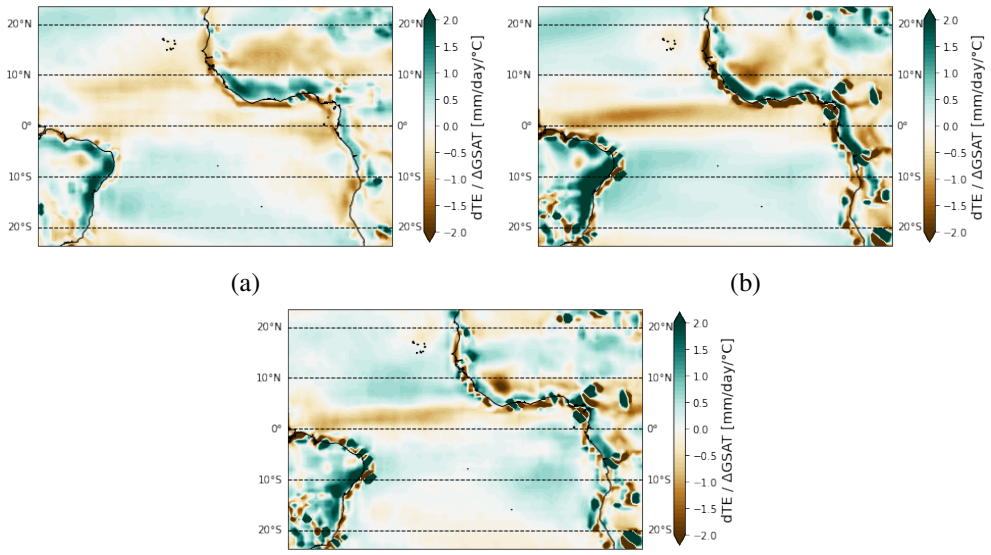

(a) (b)

(c)

Fig. 4.4 *Transient eddies contribution to the moisture budget changes for a) SAD group and b) in a LAD group. c) is the difference between a) and b). The transient eddies contribution predicted by each models is normalized by the respective ΔGSAT, thus units of measure are mm/day per degree of global warming.*

4.2.3 Moisture budget: the contributions of transient eddies and surface quantities contributions

The transient eddies term has the main effect of drying the poleward flank of the subtropics in the Northern Hemisphere and transporting moisture poleward (see **Appendix F**), and are also responsible for increased P – E at higher latitudes. Stronger changes associated with transient eddies moisture transport are localized on the coastal areas. In general, a drying effect is seen in the tropical Atlantic region for both the model's groups, even if under a small AMOC decline the effect seems to be weaker and spreads in a larger zonal band, which extends from 2-3°s and beyond 10°. When the simulated AMOC decline is stronger, the drying signal is more intense and concentrated in a narrower band, just above the equator. It intensifies while moving towards the American coast.

Surface quantities provide a negligible contribution to the net precipitation changes under a small AMOC decline scenario, while a slightly stronger contribution is expected if a strong decline occurred. Changes are especially pronounced in coastal areas and in inland regions. Indeed, as already mentioned, surface effects

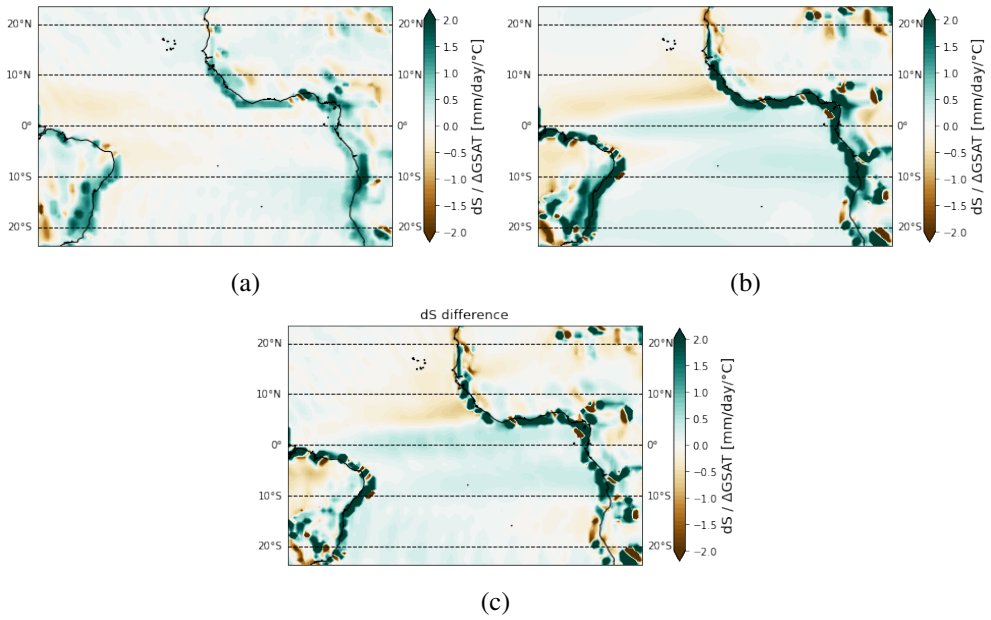

Fig. 4.5 *Surface quantities contribution to the moisture budget changes for a) SAD group and b) in a LAD group. c) is the difference between a) and b). The surface quantities contribution predicted by each models is normalized by the respective ΔGSAT, thus units of measure are mm/day per degree of global warming.*

contribution becomes relevant in proximity of significant orographic features. Given this explanation, we can better understand why their contribution above the ocean is small.

4.2.4 Comparison between the contributors and reconstruction of P - E

In **Figure 4.6** I provide bar plots that show each mechanism's contribution to the moisture budget averaged over the tropical Atlantic sector. Thus, values represent the average contribution of a grid point belonging to the tropical Atlantic region [35°W - 0°W and 4°S - 6°N]. In **Figure 4.1** the longitude-latitude box over which the averaging is performed is highlighted with black dashed lines.

Error bars indicate the corresponding inter-models uncertainties, computed as the variance of the respective values distribution for each term and for each group. Negative contributions are represented with blue bars, while positive contributions are represented by red bars. The sum of the values assumed by the bars from 1 to 4

represents the moisture budget in the tropical Atlantic, thus when they are summed result in the last bar on the right.

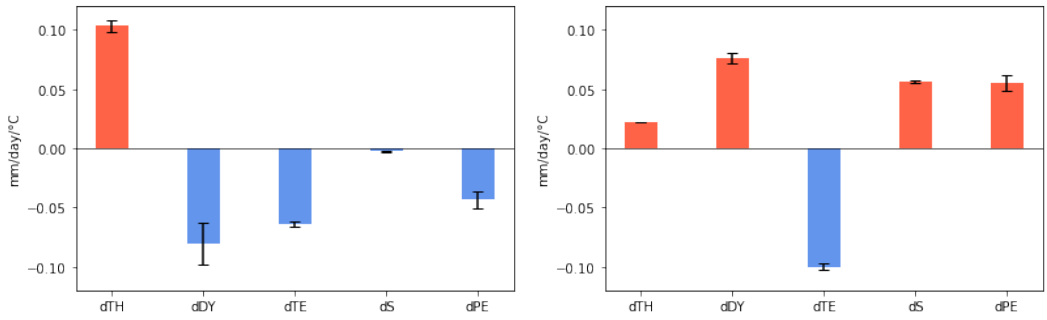

Fig. 4.6 *Bar plots with contribution of each addendum composing the moisture budget averaged on the tropical Atlantic ocean [35°W - 0°W and 4°S - 6°N] for a) SAD group and b) LAD group. The longitude-latitudes box is shown in* ***Figure 4.1****. The moisture budget contributors for each model are normalized by the respective ΔGSAT, thus units of measure are mm/day per degree of global warming.*

We note that the thermodynamic term is the only positive contribution to net precipitation changes in the SAD group. The thermodynamic mechanism gives a coherent contribution for both the sets of models. Even if the intensity of the wetting signal is lower for the SAD group, it is widely spread into the box of our interest, thus leading to an important positive contribution to the moisture budget of the small AMOC decline models. There is a high level of agreement amongst the models for the entity of the contribution of this thermodynamic term in the LAD group, whereas slightly higher uncertainties affect the SAD group.

The dynamic term provides contributions with opposite signs for the groups. As already seen in **Section 4.2.2**, the LAD group future projections show a dynamical moistening of the equatorial latitudes. The bar plot confirms this hypothesis, with a strong and positive dynamic term. Despite being coherent in sign, the dynamic term provides a larger contribution with respect to the thermodynamic one, thus prevailing on it. Although calculations are affected by a higher level of inter-model uncertainty, the dynamic term provides a negative contribution to the moisture budget of the SAD group.

Transient eddies contribution to (P-E) changes are coherent in signs, having a drying effect on the equatorial Atlantic latitudes. The effect is stronger under a large AMOC decline scenario, as was fairly visible in **Figure 4.4a** and **Figure 4.4b**. It is

also the only negative contribution to the LAD group's atmospheric moisture budget. Surface quantities do not give a relevant contribution for the SAD group, while a modest positive contribution is expected for the LAD group. Both the groups show a high level of confidence for the surface quantities contribution.

In conclusion, the net precipitation change over the tropical Atlantic ocean is regulated by different drivers. Overall, the small AMOC decline group results in negative net precipitation changes, which cannot be fully explained only by the thermodynamic and dynamic terms. In general, changes are predominantly driven by both the dynamic contributors (δDY and δTE). Thus, a drier tropical Atlantic climate is expected in the next future if AMOC will not decline massively. On the contrary, the atmospheric moisture budget over the tropical Atlantic is positive under a large AMOC decline scenario. As might be expected as a consequence of the tropical atmospheric circulation changes, both the dynamic contributors have a strong influence on the moisture budget, but with flipped signs. A slightly positive contribution of the remaining two terms leads to an average positive changes of net precipitation.

Chapter 5

Discussion and caveats

5.1 Discussion

Usually, we tend to ignore the early signals of climate change impacts whenever they seem to be far in space and time. However, results of the present work confirm that AMOC is a hotspot in a climate change context, and thus deserves special attention. The outcomes of this study broadly match those coming from similar previous studies, thus contributing to build consistency upon AMOC weakening related impacts. In addition to previous studies I provide a new moisture budget analysis of tropical precipitation change related to the AMOC decline in the Tropical Atlantic, which shows that changes in atmospheric circulation drive a southward shift in the zonal mean ITCZ but only in models projecting a relatively larger AMOC decline.

Both direct observations and CMIP6 models projections demonstrate the existence of a steady AMOC weakening trend under the effect of continuous greenhouse gas concentration rise in the atmosphere. The occurrence of an abrupt climate change due to the crossing of a tipping threshold has been largely debated [3], but according to this work and many similar studies it remains a very unlikely possibility. Nonetheless, large impacts on the whole climate system are expected as a consequence of an AMOC weakening. They clearly come out in future projections of those models that simulate the strongest AMOC decline. Consequences are expected to spread amongst the whole globe, being the AMOC closely interconnected, in a two-way

exchange, with all the other climate components, no one of which is supposed to remain untouched.

Robust statistical tests are performed to give support and reliability to the results. I evaluated whether the differences between the climate system responses to a large and to a weak AMOC decline are, in absolute value, larger than the differences predicted by two groups composed by randomly picked models amongst the available 18. When this is true, I argue that the climate responses are so distant as to be unlikely to be driven by the natural variability, thus the cause of the differences should be the AMOC decline. The temperature field is the one whose related impacts show the most recognizable patterns of change. Since AMOC transports a massive amount of heat poleward, a slowdown will cause a strong cooling in the North Atlantic region, being also affected by a positive feedback mechanism, thus accelerating at each cycle. This reduced poleward oceanic heat transport gives rise to a warming hole of sea surface temperature, that future projections mainly localize in the GIN sea.

By performing simple statistics, I discovered that, in my sample of models, AMOC reduction can explain with a high level of confidence the relative cooling of SST in the North Atlantic basin. I found that models simulating a larger AMOC decline also predict dramatically lower temperatures on the North Atlantic ocean, with respect to the SAD simulations. This cooling effect will widely spread, especially affecting the northwestern Europe climate. Thus a cooler European climate is extremely likely to occur if the AMOC underwent a strong decline. Along with temperature decrease, a drying tendency above the North Atlantic ocean, Europe and Mediterranean regions will occur. This event is not only induced by a reduced amount of water vapor into the atmosphere (caused by the temperature decrease) but other complex atmospheric-driven dynamics intervene.

However, despite large changes being expected globally, the present work mainly focuses on precipitation changes over the tropical Atlantic oceanic region, which cannot be fully attributed to temperature variations. To summarize, there exists a narrow zonal band where climatologically the trade winds converge, bringing warm and moist air, thus localizing a region of low pressure where the largest precipitation events occur, the so-called ITCZ. Under the effect of a strong AMOC decline, this band is predicted to shift from its historical mean annual positioning (5°N) equatorwards. Such migration is not predicted by models simulating a weak

AMOC decline, which instead predict an intensification of the local hydrological cycle.

By performing an atmospheric moisture budget, I discovered that the equatorial latitudes are going to be dynamically moistened, thus the southwards shift of the ITCZ is more likely to be attributed to changes in the atmospheric circulation, rather than to temperature changes. Indeed, for the strong AMOC decline group the dynamical contribution to the moisture budget is strong, and prevails over the dynamic one. Thus, modification of the climatological wind field operated by an AMOC decline in turn shapes the precipitation distribution in the tropics.

We can provide a brief explanation of how this wind field variations occur. The tropical atmospheric circulation usually acts to compensate for the oceanic heat uptake in the Southern Hemisphere and meridional transport promoted by the AMOC, by fluxing energy across the equator in the opposite direction, from the Northern Hemisphere to the Southern Hemisphere. This is achieved by enlarging and intensifying the SH Hadley cell, which is also displaced North of the equator in its annual mean. Imbalance in the inter-hemispheric heat transport would be reduced as a consequence of an AMOC slowdown, thus the mean annual southern Hadley cell would weaken too, and shift equatorwards, canceling the current asymmetry. The equatorward shifting of the ascending branches of the cells does not occur in models simulating a weak decline. It should be taken into account that the weakening and expansion of the Hadley cells, that is visible also in SAD group simulations, cannot be fully attributed to the AMOC decline, but are in general a consequence of the global warming that reduces the temperature gradient between the equator and the poles, thus enlarging and weakening the cells. This is further confirmed by the statistical tests, revailing that only differences around the equator can be considered to be very likely a response to the AMOC slowdown. However, understanding the changes of the Hadley circulation structure and intensity in response to increase in greenhouse gasses concentration, and thus in response to the interplay between the global warming and the AMOC slowdown is of crucial importance to predict the climate change associated to the subtropical dry zones and nearby areas, localized beneath the descending branch of the Hadley circulation and thus susceptible to HC location changes.

The climate response to a possible AMOC decline is an important question to be addressed, from both a societal and economic point of view. The results analyzed in

the previous sections raise concerns about the continuous anthropogenic warming. As we have seen, an AMOC weakening would put many regions under water resource stress. In fact, tropical band intensity and location are crucially important for the hydrological cycle of several areas. In particular, subtropical areas localized below the descending branch of the Hadley circulation will be subjected to a much drier climate, affecting their habitability. Many semi-arid regions may become even drier, and some deserts may expand. This phenomenon is amplified by the global warming effect, that if no atmospheric dynamics are taken into account, leads to the "dry get drier, wet get wetter mechanism". Thus, areas which already have an excess of precipitation over evaporation are expected to become even wetter, and vice versa.

Even if the analysis puts a focus on the Atlantic climate response to an AMOC slowdown, impacts are expected to be significant and persistent worldwide. Dealing with regional Hadley circulation variations, Sharmila et al. (2018) highlights how a meridional shift of the descending branch of the Hadley Cell would support a poleward displacement of the tropical-cyclone-favorable climate conditions to higher latitudes regions, increasing the related hazards. Some studies argue a shift to a more El-Niño- like climate over the Pacific ocean. Another important element that is supposed to be affected by the AMOC decline are Indian monsoons, extremely important from a societal and economic point of view. A strong AMOC decline would put many Indian regions under risk of more frequent and intense periods of drought. Through its atmospheric teleconnections AMOC is also supposed to communicate with the southern mid-latitudes, and thus leading to an increase of westerlies and wind stress over the Southern Ocean. [31]

5.2 Conclusions

Given the high complexity of the interconnections between AMOC and the other climate components, a faithfully computerized representation of its mass and energy exchange across time and space is still a major issue for CMIP6 models. Weijier et al. (2020) assessed that "AMOC decline in CMIP6 is surprisingly insensitive to the scenario at least up to 2060." As explained in **Section 2.3.2**, and further demonstrated in **Appendix B**, some biases are already present in the AMOC's historical representation, and further spread with the passing of simulated time. As a result, a even larger inter-model spread affects the representation of the AMOC

intensity in future projections. This bias makes it extremely difficult to perform precise predictions about the future climate over the North Atlantic ocean region, and result in a major source of uncertainty for this type of analysis.

In the present study, I make a comparison between future projections extrapolated by models which simulate the strongest decline, and future projections predicted by the models simulating the weakest decline. For the work I selected all the CMIP6 models that had submitted the overturning streamfunction variable for both the historical run and the SSP585 future projection (spanning between 1850 and 2100). I came up with a sample of 18 models. Thus, the two sets of models under analysis are composed of only 6 models each, often coming from the same modeling center, and thus probably affected by the same biases. As already mentioned, performing MMEs reduces errors and increases the consistency of the results. However, if models are affected by the same bias, there is a high probability that the bias is amplified by the MME, especially if the number of models amongst which the ensemble is performed is small. For a future analysis, more models coming from different modeling centers can be used to improve the reliability and accuracy of the results and obtain more truthful information. As already pointed out by Bellomo et al. (2021), another effort that should be done to improve accuracy and reliability to the study is related to the necessity of finding a method to better isolate the climate response to an AMOC slowdown from the general climate responses to the climate change.

Another caveat to this study derives from the limited duration of the simulations. As previously mentioned, extended simulations reaching year 2300 show the AMOC's intensity reaching a plateau, and thus stabilizing. However, as we saw in **Figure 2.2**, between years 2071 and 2100 the AMOC is still declining at a sustained rate, thus is in a transient state. Hence, we cannot be exhaustive in the analysis of climate system response, since the AMOC's decline has not yet completely developed and reached a stability. To fully catch the AMOC's decline consequences we would need equilibrated simulations.

Even if similar studies have been conducted, the majority of them force the climate models to induce an AMOC collapse or slowdown, usually by adding freshwater fluxes in the Labrador Sea/Northern Atlantic close to Greenland.. This study is meant to build upon our knowledge about the effects climate change may have on the AMOC, which is an essential component of the entire climate system. Thus, a major difference with respect to similar previous studies is that for this

analysis, instead of artificially triggering an AMOC slowdown, I use SSP585 future scenario projections, and let the AMOC evolve (and decline) under the continuous greenhouse gasses concentration rise. Thus AMOC naturally responds to the global warming, to the decline of sea ice, to anomalous atmospheric circulation, and all the other climate changes driven by anthropogenic emissions. The SSP585 scenario is the "worst case" scenario developed to understand climate system change as a response to continuous and totally uncontrolled greenhouse gas emissions.

References

[1] Zhang, R. et al. A review of the role of the Atlantic meridional overturning circulation in Atlantic multidecadal variability and associated climate impacts. Rev. Geophys. 57, (2019). 316–375 https://doi.org/10.1029/2019RG000644

[2] Weijer, W., Cheng, W., Garuba, O., Hu, A. Nadiga, B. CMIP6 models predict significant 21st century decline of the Atlantic meridional overturning circulation. Geophys. Res. Lett. 47, e2019GL086075. (2020). https://doi.org/10.1029/2019GL086075

[3] Sgubin, G., Swingedouw, D., Drijfhout, S. et al. Abrupt cooling over the North Atlantic in modern climate models. Nat Commun 8, 14375 (2017). https://doi.org/10.1038/ncomms14375

[4] Stouffer R. J. et al. Investigating the causes of the response of the thermohaline circulation to past and future climate changes J. Clim. 19 1365–87. (2006) https://doi.org/10.1175/JCLI3689.1

[5] Brodeau, L. and Torben Koenigk. Extinction of the northern oceanic deep convection in an ensemble of climate model simulations of the 20th and 21st centuries. Climate Dynamics 46: 2863-2882. (2015) https://doi.org/10.1007/s00382-015-2736-5

[6] Swingedouw J. D. et al. AMOC recent and future trends: A Crucial Role for Oceanic Resolution and Greenland Melting? Front. Clim. (2022) https://doi.org/10.3389/fclim.2022.838310

[7] Cheng, X., Tung, KK. Global surface warming enhanced by weak Atlantic overturning irculation. Nature 559, 387–391 (2018). https://doi.org/10.1038/s41586-018-0320-y

[8] Michel, S.L.L., Swingedouw, D., Ortega, P. et al. Early warning signal for a tipping point suggested by a millennial Atlantic Multidecadal Variability reconstruction. Nat Commun 13, 5176 (2022). https://doi.org/10.1038/s41467-022-32704-3

[9] Zhang, R. and Delworth, T. L. Simulated tropical response to a substantial weakening of the Atlantic thermohaline circulation. J. Clim. 18, 1853–1860 (2005). https://doi.org/10.1175/JCLI3460.1

[10] Jackson, L. C. et al. Global climate impacts of a slowdown of the AMOC in a high resolution GCM. Clim. Dyn. 45, 3299–3316 (2016). https://doi.org/10.1007/s00382-015-2540-2

[11] Kim, SK., Kim, HJ., Dijkstra, H.A. et al. Slow and soft passage through tipping point of the Atlantic Meridional Overturning Circulation in a changing climate. npj Clim Atmos Sci 5, 13 (2022). https://doi.org/10.1038/s41612-022-00236-8

[12] Schmidt, D. F., and Grise, K. M. The response of local precipitation and sea level pressure to Hadley cell expansion. Geophysical Research Letters,44,10,573–10,582. (2017). https://doi.org/10.1002/2017GL075380

[13] Cheng, W., MacMartin, D.G., Kravitz, B. et al. Changes in Hadley circulation and intertropical convergence zone under strategic stratospheric aerosol geoengineering. npj Clim Atmos Sci 5, 32 (2022). https://doi.org/10.1038/s41612-022-00254-6

[14] Frierson, D., Coauthors. Contribution of ocean overturning circulation to tropical rainfall peak in the Northern Hemisphere. Nat. Geosci. 6, 940–944 (2013). https://doi.org/10.1038/ngeo1987

[15] Marshall, J., Donohoe, A., Ferreira, D. et al. The ocean's role in setting the mean position of the Inter-Tropical Convergence Zone. Clim Dyn 42, 1967–1979 (2014). https://doi.org/10.1007/s00382-013-1767-z

[16] Gosling, S. The likelihood and potential impact of future change in the large-scale climate-earth system on ecosystem services. Environmental Science Policy 27:S15-S31 (2013). https://doi.org/10.1016/j.envsci.2012.03.011.

[17] Sevellec, F., Fedorov, A. V. and Liu, W. Arctic sea-ice decline weakens the Atlantic meridional overturning circulation. Nat. Clim. Change 7, 604–610 (2017). 10.1007/s00382–015–2915–4

[18] Keil, P. et al. Multiple drivers of the North Atlantic warming hole. Nat. Clim. Change 10, 667–671 (2020). https://doi.org/10.1038/s41558-020-0819-8

[19] Kageyama, M., Merkel, U., Otto-Bliesner, B., Prange, M., Abe-Ouchi, A., Lohmann, G., Ohgaito, R., Roche, D. M., Singarayer, J., Swingedouw, D., and X Zhang: Climatic impacts of fresh water hosing under Last Glacial Maximum conditions: a multi-model study, Clim. Past, 9, 935–953 (2013). https://doi.org/10.5194/cp-9-935-2013

[20] Allen, R. J. A 21st century northward tropical precipitation shift caused by future anthro-pogenic aerosol reductions. J.Geophys. Res. Atmos.,120, 9087–9102. (2015). https://doi.org/10.1002/2015JD023623

[21] Tebaldi, C., Knutti, R. The use of the multi-model ensemble in probabilistic climate projections. Philos. Transact. A Math. Phys. Eng. Sci. 365, 2053–2075. (2007). https://doi.org/10.1098/rsta.2007.2076

[22] Mitevski, I., Orbe, C., Chemke, R., Nazarenko, L., and Polvani, L. M. Non-monotonic response of the climate system to abrupt CO_2 forcing. Geophysical Research Letters, 48, e2020GL090861, (2021). https://doi.org/10.1029/2020GL090861

[23] Wei, L., Alexey F. and Florian S. The mechanisms of the Atlantic meridional overturning circulation slowdown induced by Arctic sea ice decline. Journal of Climate, 32 (4), 977-996. (2019). https://doi.org/10.1175/JCLI-D-18-0231.1

[24] O'Neill, B. C., Tebaldi, C., van Vuuren, D. P., Eyring, V., Friedlingstein, P., Hurtt, G., Knutti, R., Kriegler, E., Lamarque, J.-F., Lowe, J., Meehl, G. A., Moss, R., Riahi, K., and Sanderson, B. M.: The Scenario Model Intercomparison Project (ScenarioMIP) for CMIP6, Geosci. Model Dev., 9, 3461–3482. (2016). https://doi.org/10.5194/gmd-9-3461

[25] Bellomo, K., Angeloni. M., Corti, S., von Hardenberg, J. Future climate change shaped by inter-model differences in Atlantic meridional overturning circulation response. Nat Commun. Jun 16; 12(1):3659. (2021). https://doi.org/10.1038/s41467-021-24015-w

[26] L Huusko, L., Bender, F., Annica, M. L. and Storelvmo, T. Climate sensitivity indices and their relation with projected temperature change in CMIP6 models. Environ. Res. Lett. 16 064095 (2021). 10.1088/1748-9326/ac0748

[27] Carvalho-Oliveira, J., Borchert, L. F., Duchez, A., Dobrynin, M., Baehr, J. Subtle influence of the Atlantic Meridional Overturning Circulation (AMOC) on seasonal sea surface temperature (SST) hindcast skill in the North Atlantic. Weather and Climate Dynamics, Copernicus, 2, pp.739-757 (2021). https://doi.org/10.5194/wcd-2-739-2021

[28] Vellinga, M. and Wood, R. A. Impacts of thermohaline circulation shutdown in the twenty-first century. Clim. Change 91, 43–63 (2008). https://doi.org/10.1007/s10584-006-9146-y

[29] Gervais, M., Shaman, J. and Kushnir, Y. Mechanisms gverning the development of the North Atlantic warming hole in the CESM-LE future climate simulations. J. Clim. 31, 5927–5946, (2018). https://doi.org/10.1175/JCLI-D-17-0635.1

[30] Marzocchi, A et al. The North Atlantic subpolar circulation in an eddy-resolving global ocean model. Journal of Marine Systems, 142, Pages 126-143. (2015). https://doi.org/10.1016/j.jmarsys.2014.10.007

[31] Shih-Yu, L. et al, Southern Ocean wind response to North Atlantic cooling and the rise in atmospheric CO2: Modeling perspective and paleoceanographic implications. American Geophysical Union (AGU). (2011). https://doi.org/10.1029/2010PA002004

[32] Jackson, L. C., and Wood, R. A. Hysteresis and resilience of the AMOCin an eddy-permitting GCM.Geophys-ical Research Letters,45, 8547–8556. (2018). https://doi.org/10.1029/2018GL078104

[33] Seager, R., Naik, N. and Vecchi, G. A. Thermodynamic and dynamic mechanisms for large-scale changes in the hydrological cycle in response to global warming. J. Clim. 23, 4651–4668 (2010). https://doi.org/10.1175/2010JCLI3655.1

[34] Sharmila, S., Walsh, K.J.E. Recent poleward shift of tropical cyclone formation linked to Hadley cell expansion. Nature Clim Change 8, 730–736 (2018). https://doi.org/10.1038/s41558-018-0227-5

[35] Held, I. M. and Soden, B. J. Robust responses of the hydrological cycle to global warming. J. Clim. 19, 5686–5699 (2006). https://doi.org/10.1175/JCLI3990.1

[36] Kevin, E., Trenberth., Christian, J., Guillemot. Evaluation of the Global Atmospheric Moisture Budget as Seen from Analyses. Journal of Climate, 8(9):2255-2272. (1995) https://doi.org/10.1175/1520-0442

[37] D'Agostino, R. and Lionello, P., The atmospheric moisture budget in the Mediterranean: Mechanisms for seasonal changes in the Last Glacial Maximum and future warming scenario. Quaternary Science Reviews, Volume 241, article id. 106392. (2020). https://doi.org/10.1016/j.quascirev.2020.106392

[38] Wang, Z., A. Duan, S. Yang, and K. Ullah, Atmospheric moisture budgetand its regulation on the variability ofsummer precipitation over the Tibetan Plateau, J. Geophys. Res. Atmos.,122,614–630. (2017). https://doi.org/10.1002/2016JD025515

[39] Wassenburg, J. A., Vonhof, H. B., Cheng, H., Martínez-García, A., Ebner, P. R., Li, X., Zhang, H., Sha, L., Tian, Y., Edwards, R. L., Fiebig, J., and Haug, G. H. Penultimate deglaciation Asian monsoon response to North Atlantic circulation collapse. Nature Geoscience, 14(12), 937-941. (2021). https://doi.org/10.1038/s41561-021-00851-9

[40] De Toma, V.; Artale, V. Yang, C. Exploring AMOC Regime Change over the Past Four Decades through Ocean Reanalyses. Climate 2022, 10, 59. (2022). https://doi.org/10.3390/cli10040059

Appendix A

Statistical tests

Differences between historical and future temperature and precipitation fields

I perform a two-tailed statistical test assuming equal variance on the temperature and precipitation field anomalies between the historical datasets and the future ones, for each model. Stipplings indicate where the tests revealed there have been no statistically relevant changes.

For the temperature field (**Figure A.1**), many models predict relevant changes for each grid point, thus here are not shown. Notice that non-relevant changes are mainly localized at the coordinates interested by the rise of the NAWH, or around it. This region is characterized by a slower temperature warming rate than the rest of the globe, thus it is not surprising that some changes are small if compared to the historical climate. Some models also predict non-relevant temperature changes in the Weddell and Ross sea, where a reduced warming is generally associated with a decrease in the mixed layer depth, behaving similarly to the North Atlantic region.

I also perform a statistical test on the precipitation distribution (**Figure A.2**). Since it is spatially highly dishomogeneous, and does not undergo a sort of linear increasing trend as happens with temperature increase, in this analysis I use a slightly lower significance level (85%). For all the models, a large portion of precipitation distribution over the globe is going to change with the ongoing climate change. Given the complex dynamics and the massive quantity of factors that may

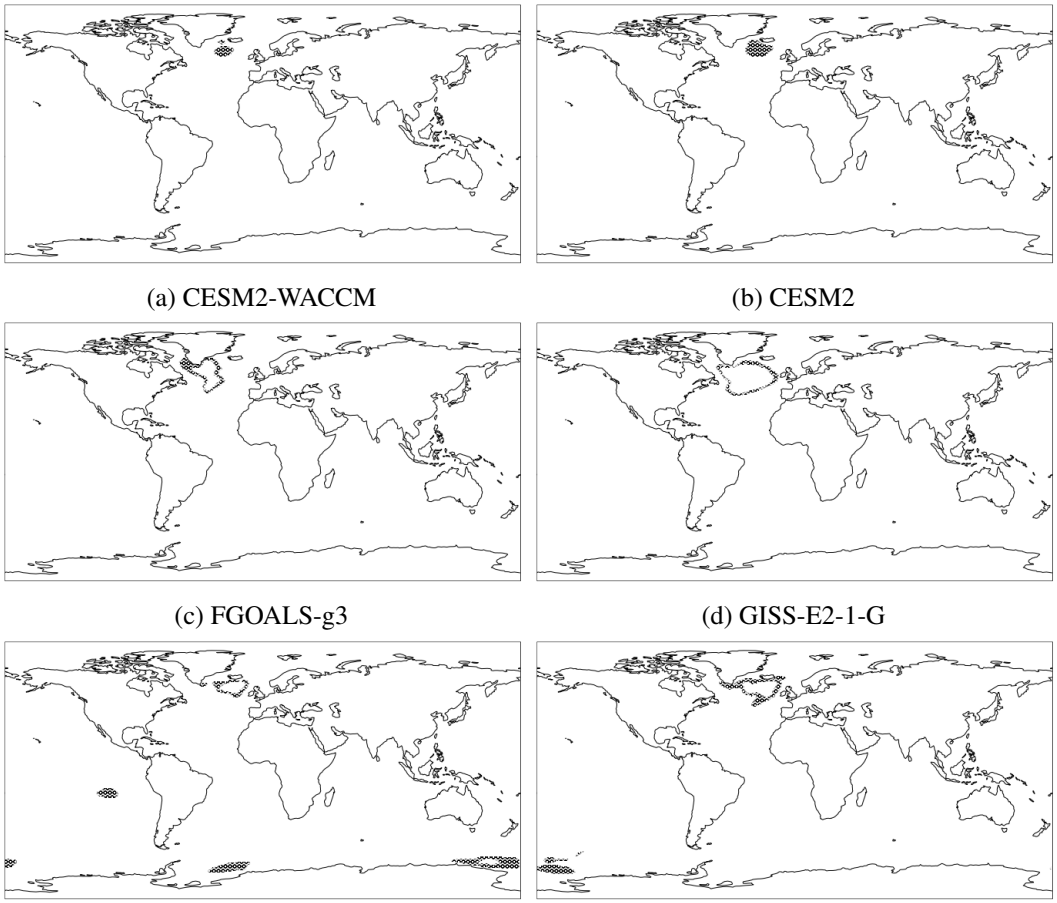

(a) CESM2-WACCM (b) CESM2

(c) FGOALS-g3 (d) GISS-E2-1-G

(e) NorEMS2-LM (f) NorEMS2-MM

Fig. A.1 *Stippling indicate where the future temperature field does not show statistically relevant changes with respect to the past climate.*

determine precipitation changes on a global-scale, it is more difficult to understand why in certain areas the precipitation distribution varies with respect to the historical simulation while in other areas precipitation changes seem to lie within the natural variability of the climate system. However, the majority of the models reveal relevant changes for the tropical Atlantic region, which is the area on which this work is mainly focused.

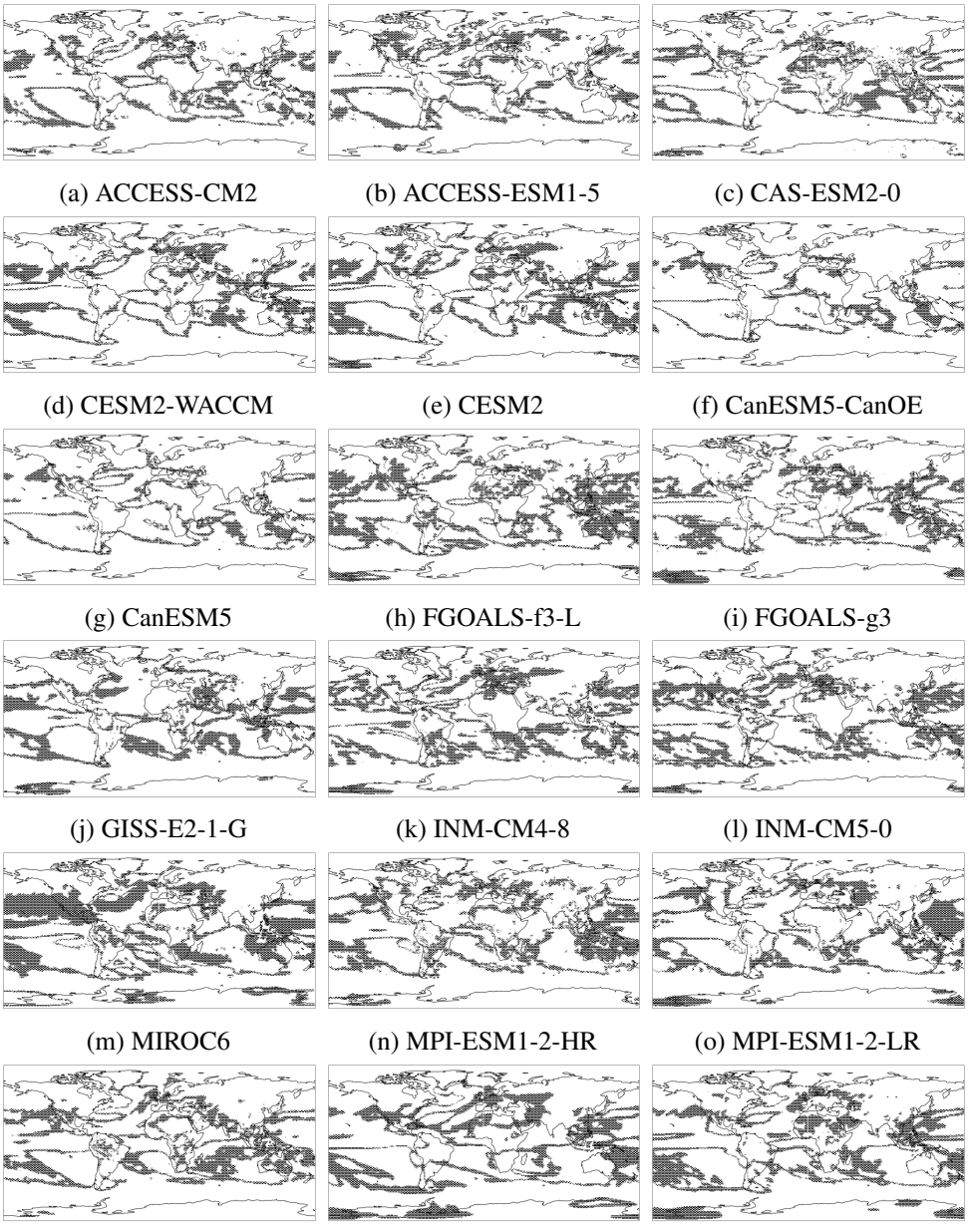

(a) ACCESS-CM2 (b) ACCESS-ESM1-5 (c) CAS-ESM2-0

(d) CESM2-WACCM (e) CESM2 (f) CanESM5-CanOE

(g) CanESM5 (h) FGOALS-f3-L (i) FGOALS-g3

(j) GISS-E2-1-G (k) INM-CM4-8 (l) INM-CM5-0

(m) MIROC6 (n) MPI-ESM1-2-HR (o) MPI-ESM1-2-LR

(p) MRI-ESM2-0 (q) NorESM2-LM (r) NorESM2-MM

Fig. A.2 *Stippling indicate where the future precipitation field does not show statistically relevant changes with respect to the past climate.*

Appendix B

Complete time-series of AMOC (1850 - 2100)

Figure B.1 shows the time series of AMOC's intensity predicted by all the models, spanning the years between 1850 and 2100. No low pass filters have been applied to allow the visualization of AMOC's periodic oscillations.

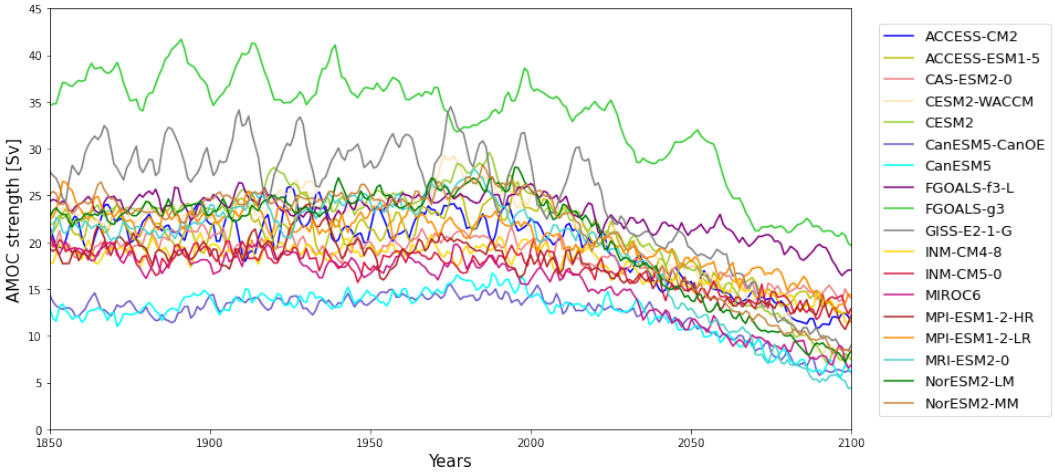

Fig. B.1 *Time series of AMOC predicted by the 18 models of our sample.*

Results largely agree on some previous findings:

- There is evidence of the extremely large inter-model spread in AMOC historical representation, with model FGOALS-g3 model simulating the strongest historical intensity (with an average value of 34 Sv at the end of the 20^{th}

century), and CanESM5 model providing the lowest one (with an average value of 15 Sv at the end of the 20^{th} century).

- All models show the natural variability of AMOC strength. However, there is no common agreement about the periodicity of the oscillations affecting the AMOC strength between the models. As well, the amplitude of such oscillations largely varies among the simulations. In accordance with previous findings, the oscillations' amplitudes linearly depend on the mean strength of the AMOC in the historical simulation, thus models simulating a stronger AMOC intensity also show larger amplitudes. [2] [25]

- Figure visually confirms that a higher declining rate in AMOC strength for many models began in the late 1990s. At the end of the 21^{st} century, a plateau has yet not been reached by any of the simulations.

Appendix C

Mixed Layer Depth changes

The Labrador Sea is the oceanic region where near-surface oceanic currents lose heat to the overlying atmosphere, thus become denser, and sink at depth. [39] For these dynamics the Labrador Sea Waters are considered a key component of the AMOC, since they sustain the return flow of the bottom branch (NADW) towards lower latitudes. However, the convective mixing that connects surface currents to the deep currents is strongly sensitive to both surface water and deep water conditions. [40] These are in turn affected by freshwater fluxes from Greenland and Arctic gates' ice sheets melting. Both surface melt and glacier discharge play a role in changing the freshwater budget of the subarctic Atlantic ocean. The surface water freshening leads to an increase of water stratification, which in turn reduces the formation of the deep water. [29]

The Mixed Layer Depth (MLD) is a classic diagnostic method for detecting the deep water convective activity [3]. Even if the picture shows some noise, the MLD difference between the two groups of models clearly shows a larger MLD reduction in the LAD group (variation of MLD is obtained as MLD_{SAD} minus MLD_{LAD}, thus positive values are associated to a thinner MLD for the LAD group). These differences are mostly pronounced in the Labrador sea, and spreads below Greenland, within the subpolar gyre.

The progressively reduction of MLD in the Labrador Sea suggests the weakening of the deep convection activity in this area. The fact that this MLD thinning is more pronounced for those models classified as large AMOC decline, further confirms the

goodness of the models division. Simulated MLD thickness difference between the two sets of models ranges between 200m and 300m.

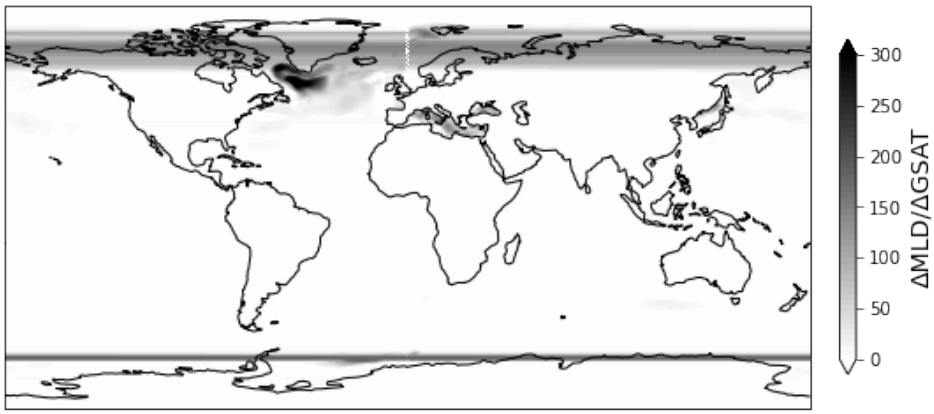

Fig. C.1 *Mixed layer depth variation differences between SAD and LAD (SAD minus LAD). Units of measure are m per degree of global warming*

Noise in the picture do not allow us to appreciate a similar deepening signal occurring in the Weddel and Ross sea, just above the Antarctica region, where the NADW originates.

For models INM-CM4-8 and INM-CM5-0 the mlotst variable (mixed layer depth) dataset was not available for the experiments under analysis, so they have been excluded from the analysis. Thus, the ensemble mean amongst the small AMOC decline group only accounts for the remaining 4 models.

Appendix D

Evaporation changes

The evaporation phenomenon is of extreme importance for the climate system, since it regulates the amount of water vapor in the atmosphere, and thus affects the water cycle. With the widespread anthropogenic warming, the evaporation rate is expected to increase worldwide, as more heat would be available in the atmosphere, and thus more water could experience the phase transition, as described by the Clausius Clapeyron equation.

Sections 3.1 and **Section 3.2** suggested that the temperature field would experience a strong cooling over the region interested by the NAWH as a response to a large AMOC slowdown, while the mean annual precipitation is going to decrease. Coherently, the evaporation changes show a unique behavior in the same region, with negative values, linked to the reduction of near surface temperature, thus leading to a lower amount of water vapor in the atmosphere.

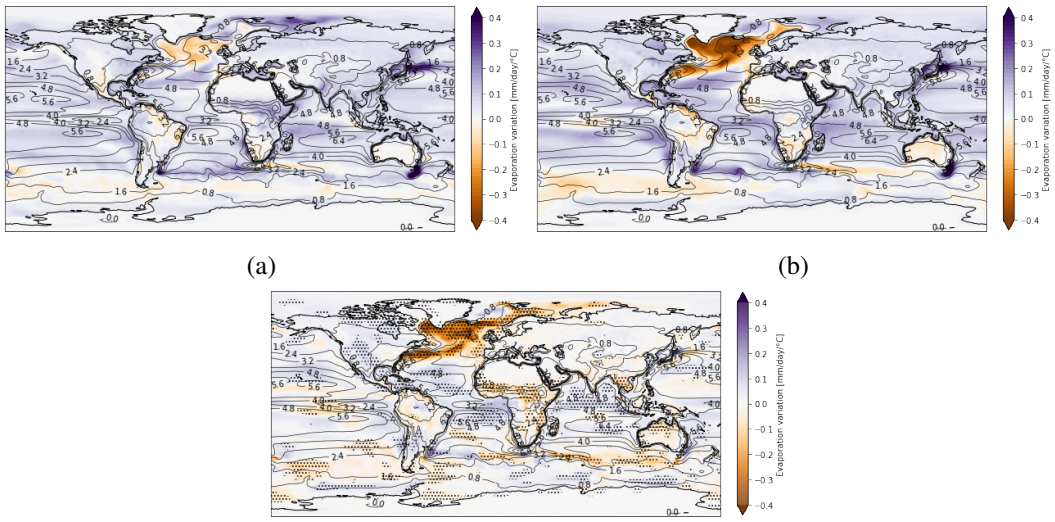

(a) (b)

(c)

Fig. D.1 *Evaporation anomalies for a) SAD group and b) LAD group. Superimposed black contours represent the mean climatology computed from all the 18 models. The evaporation variation predicted by each models is normalized by the respective ΔGSAT, thus units of measure are mm/day per degree of global warming. Figure c) is the difference between a) and b). Stippling indicates where the difference between LAD and SAD groups is statistically significant at the 95% threshold.*

Appendix E

Austral winter Hadley cells changes

In the DJF, the small AMOC decline group shows a meridional expansion for both the cells, with anomalies whose sign is coherent with the rotational direction of the wind. So if we look at panel a, We can clearly see a weakening of the SH cell (red area between 40°S and 20°S), with an expansion tendency. For the NH cell the effects are the same, thereby weakening and expansion (anomalies have flipped sign with respect to the SH cell), thus compressing the mid-latitudes cell. For the large AMOC decline group, there is a clear clockwise anomaly between 0°N and 5°N that can be both associated to a shifting of the NH cell equatorward and to a weakening of the SH cell. Both the cells further weaken while moving poleward.

Statistical tests suggest that the differences between the boreal winter cell anomalies are statistically relevant between 20°S and 20°N, thus confirming that the NH cell equatorwards shift and SH weakening can be attributed to the AMOC decline.

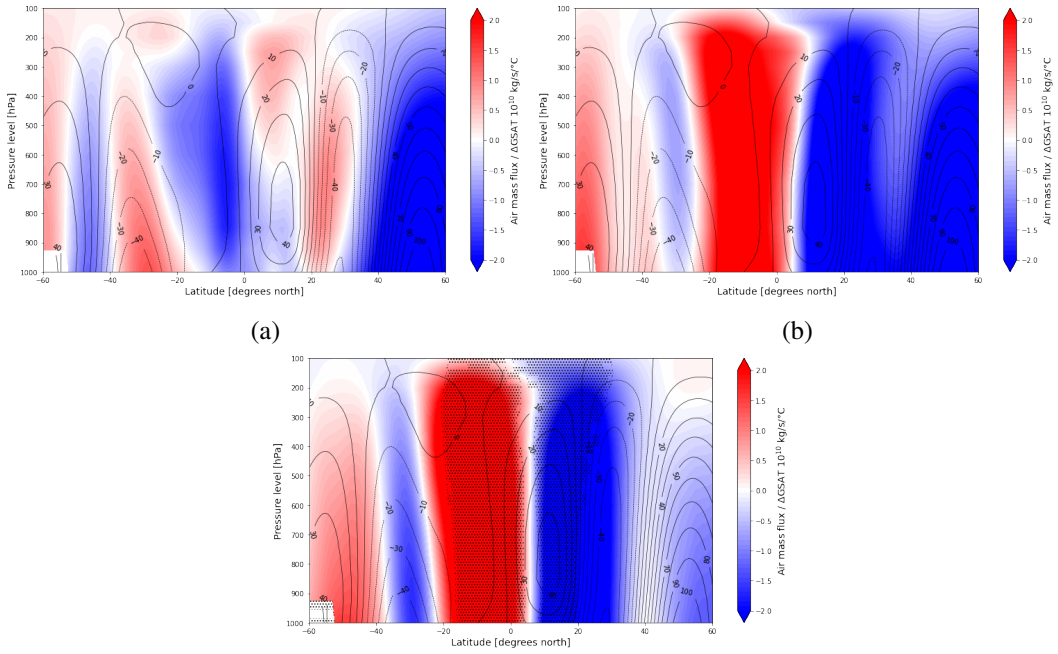

Fig. E.1 *Tropical Atlantic Hadley circulation anomalies in boreal winter season (JJA) in a) SAD scenario and b) LAD scenario. Panel c) is the difference between the two. Superimposed black contours represent the mean seasonal climatology. Negative values indicate an anti-clockwise circulation, while positive values correspond to a clockwise one. The atmospheric circulation variation predicted by each models is normalized by the respective ΔGSAT, thus units of measure are* $10^{10}\ \frac{kg}{s}$ *per degree of global warming. Stippling indicates where the difference is statistically significant at the 90% threshold Stippling indicates where the difference is statistically significant at the 90% threshold.*

Appendix F

Moisture budget - global results

Thermodynamic term

As previously pointed out, the thermodynamic term is constrained by the Clausius Clapeyron relation. Since a warming climate will lead to an increase of water vapor into the atmosphere, imagining a fixed circulation, the transport of water vapor would intensify, following the increase of specific humidity. Thus, the spatial pattern of P-E change caused by the thermodynamic driver would remain unchanged, as confirmed by the similarities between **Figure F.1a** and **Figure F.1b**. However, here values differ between the two sets of models mainly because of the different projected temperature field analyzed in **Section 3.1** (thus slightly warmer temperature for the LAD group in the deep tropics, and cooler temperature in the NA and subpolar NA regions, particularly pronounced over the NAWH).

Dynamic term

Main net precipitation changes caused by the dynamic contributor are localized in the deep tropics, accounting for positive changes spread over the tropical Pacific. Some drying contributions are localized at the subtropical latitudes. These are more intense for the SAD group, and may be due to the expansion of the Hadley cells discussed in **Section 3.3**, and a poleward shift of the mid-latitude storm tracks. Some negative anomalies of net precipitation are predicted over the Philippines and Southern Indian ocean, by both the groups. Note that dynamic contributor is also responsible for the strengthening of the Indian Monsoons in both the scenarios. The moistening signal is stronger and larger in the SAD group. This is totally coherently with the observation performed in **Section 3.2**, according to which the precipitation increase in

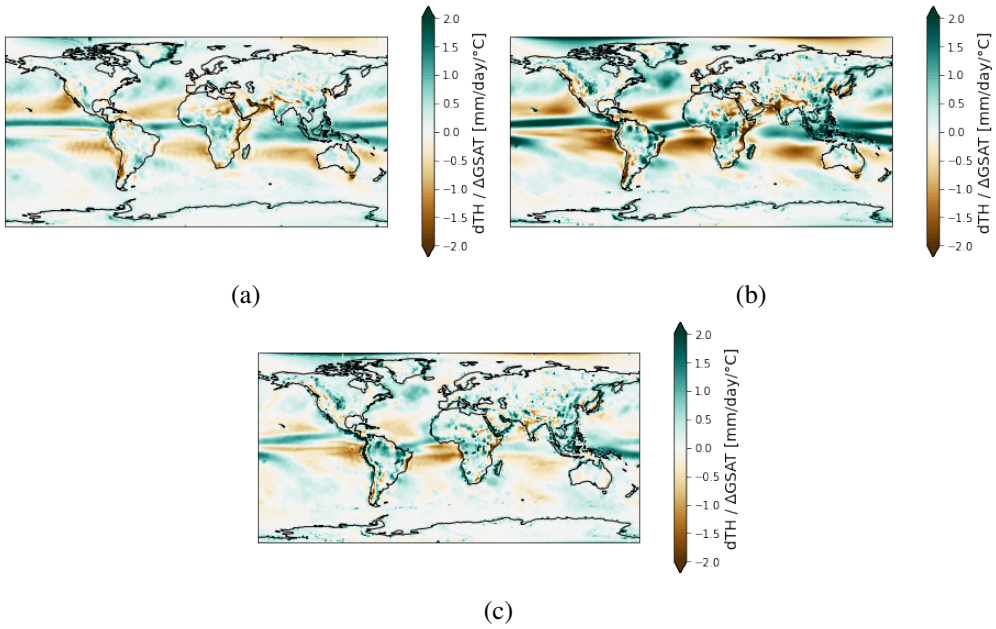

(a) (b)

(c)

Fig. F.1 *Thermoynamic contribution to the moisture budget changes for a) SAD group and b) LAD group. Figure c) is the difference between a) and b). Units of measure are mm/day per degree of global warming.*

a LAD scenario is weaker than the precipitation increase predicted by the SAD group.

Transient eddies term

In general, the contribution to the moisture budget of the transient eddies tends to dry the poleward flank of the subtropics and moisten the higher latitudes [33]. Effects are mainly pronounced close to the coastal areas. The signal is stronger in a LAD scenario.

Surface quantities term

The effects linked to surface quantities are mainly localized on coastal areas, mainly caused by the presence of significant orographic features. An extremely poor contribution is expected over the oceanic regions.

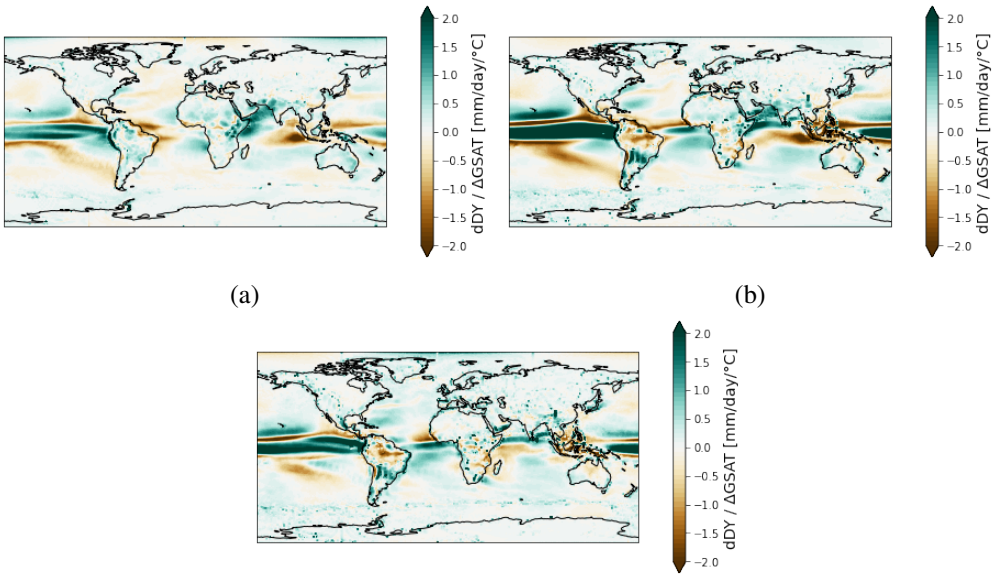

(a) (b)

(c)

Fig. F.2 *Dynamic contribution to the moisture budget changes for a) SAD group and b) LAD group. Figure c) is the difference between a) and b). Units of measure are mm/day per degree of global warming.*

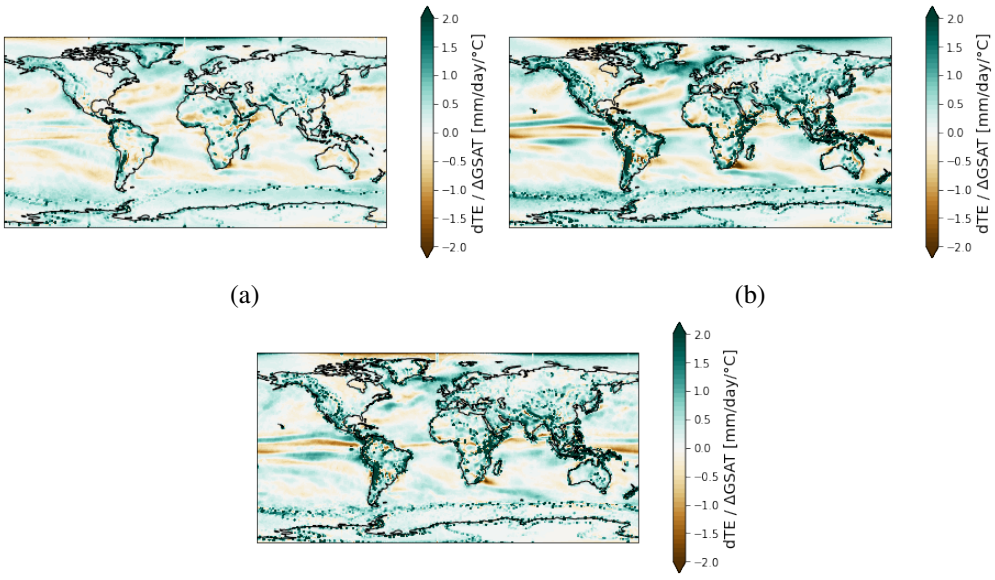

(a) (b)

(c)

Fig. F.3 *Transient eddies contribution to the moisture budget changes for a) SAD group and b) LAD group. Figure c) is the difference between a) and b). Units of measure are mm/day per degree of global warming.*

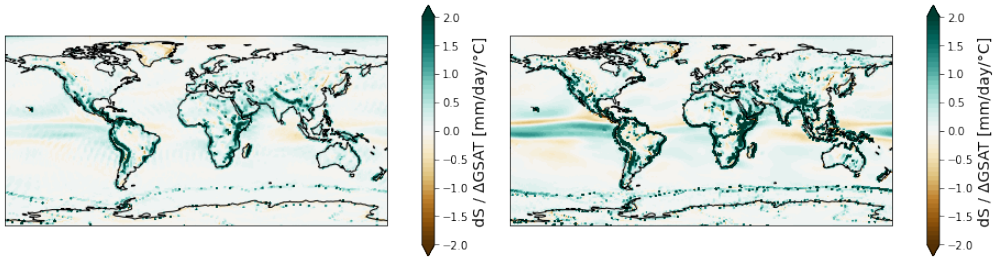

(a)

(b)

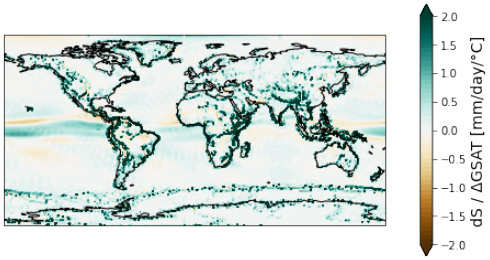

(c)

Fig. F.4 *Surface quantities contribution to the moisture budget changes for a) SAD group and b) LAD group. Figure c) is the difference between a) and b). Units of measure are mm/day per degree of global warming.*